AD_____

Award Number: W81XWH-05-C-0004

TITLE: Targeted Therapies for Myeloma and Metastatic Bone Cancers

PRINCIPAL INVESTIGATOR: Dr. Neal Vail

CONTRACTING ORGANIZATION: Southwest Research Institute
San Antonio, TX 78238

REPORT DATE: September 2010

TYPE OF REPORT: Final

PREPARED FOR: U.S. Army Medical Research and Materiel Command
Fort Detrick, Maryland 21702-5012

DISTRIBUTION STATEMENT: Approved for public release; distribution unlimited

# REPORT DOCUMENTATION PAGE

*Form Approved*
*OMB No. 0704-0188*



| **1. REPORT DATE** *(DD-MM-YYYY)* | **2. REPORT TYPE** | **3. DATES COVERED** *(From - To)* |
|---|---|---|
| 01-09-2010 | Final | 18 JAN 2005 - 31 AUG 2010 |

**4. TITLE AND SUBTITLE**
Targeted Therapies for Myeloma and Metastatic Bone Cancers

**5a. CONTRACT NUMBER**

**5b. GRANT NUMBER**
W81XWH-05-C-0004

**5c. PROGRAM ELEMENT NUMBER**

**6. AUTHOR(S)**
Dr. Neal Vail

E-Mail: gianny.rossini@swri.org

**5d. PROJECT NUMBER**

**5e. TASK NUMBER**

**5f. WORK UNIT NUMBER**

**7. PERFORMING ORGANIZATION NAME(S) AND ADDRESS(ES)**
Southwest Research Institute
San Antonio, TX 78238

**8. PERFORMING ORGANIZATION REPORT NUMBER**

**9. SPONSORING / MONITORING AGENCY NAME(S) AND ADDRESS(ES)**
U.S. Army Medical Research and Materiel Command
Fort Detrick, Maryland 21702-5012

**10. SPONSOR/MONITOR'S ACRONYM(S)**

**11. SPONSOR/MONITOR'S REPORT NUMBER(S)**

**12. DISTRIBUTION / AVAILABILITY STATEMENT**
Approved for Public Release; Distribution Unlimited

**13. SUPPLEMENTARY NOTES**

**14. ABSTRACT**
Abstract on next page.

**15. SUBJECT TERMS**
Bone targeted nanoparticles, bone cancer myeloma, mice studies, PLGA, Biodegradable materials.

| **16. SECURITY CLASSIFICATION OF:** | | | **17. LIMITATION OF ABSTRACT** | **18. NUMBER OF PAGES** | **19a. NAME OF RESPONSIBLE PERSON** |
|---|---|---|---|---|---|
| **a. REPORT** | **b. ABSTRACT** | **c. THIS PAGE** | | | USAMRMC |
| U | U | U | UU | 73 | **19b. TELEPHONE NUMBER** *(include area code)* |

**14. ABSTRACT**

Performed *in-vivo* efficacy diseased and normal mice

**Propose:** To demonstrate *in-vivo* efficacy of bone-targeted nanoparticles loaded with Velcade in a mouse model of bone myeloma.
**Scope:** Test of 0.2 and 1% loading (Velcade) targeted and non-targeted; 5% PEG coated nanoparticles in GFP-Myeloma *in-vivo* model.
**Major findings:** Both classes of NPs tested (targeted and non-targeted) exhibit anti-tumor efficacy in the murine 5TGM1 model of multiple myeloma. (Data in Appendix; subcontract to UTHSCSA Dr Babatunde O. Oyajobi, M.D., Ph.D.)

Demonstrated bone biodistribution in diseased and normal mice

**Propose:** To demonstrate preferential bone distribution of bone-targeted NPs.
**Scope:** We tested 5% and 15% PEG NPs targeted and non-targeted in control and diseased mice (Myeloma).
**Major findings:** We demonstrated partial bone accumulation of the targeted nanoparticles *in vivo.* No preferential accumulation (significant) was detected with targeted over non-targeted NPs. (Fig 14-19)

Quantified functional groups available for ligand conjugation using OPA reagent

**Propose:** To demonstrate and quantify ASP4 bone targeting functional groups in NPs.
**Scope:** OPA reagent followed by amino-acid quantification using plate reader was done on NPs after acid hydrolysis to quantify ASP4 ligand in targeted and control NPs.
**Major findings:** We were able to directly quantify the ligand (ASP4) and results were consistent with the expected results (Appendix 3).

Quantified functional groups available for ligand conjugation using $S^{35}$-labeled ligands

**Propose:** To develop a technique to measure the presence of functional maleimide in the NPs surface.
**Scope:** Use of radiotracer cysteine amino acid [$S^{35}$] to conjugate to functional maleimide group on the NP surface. Follow up by competition of labeling with cold cysteine.
**Major findings:** We demonstrated the presence of functional Maleimide in NPs surface. (Data shown on previous report)

Developed alternative assay to confirm affinity of bone-targeting nanoparticles to hydroxyapatite substrates

**Propose:** To demonstrate bone targeting *in-vitro* using alternative tracer, this should help to confirm the binding assay is correct and not due to the tracer and carrier protein used with the tracer.
**Scope:** We encapsulated a hydrophobic dye (rhodamine) using similar NP preparation procedures without a protein carrier.
**Major findings:** *In-vitro* binding results using the dye were similar to the results with the radioactive tracer; this confirms the binding is not due to the procedure used or the carrier protein. (Fig 10)

Demonstrated *in-vitro* stability of radio-labeled nanoparticles

**Propose:** To develop methods to radio-label NPs. Current methods in the literature were tested but found to be incompatible with NP work for our studies.
**Scope:** Conjugation to a carrier protein followed by loading into NPs was investigated.
**Major findings:** The optimized procedure was shown to be effective in terms of stability of label, and time to produce NPs for *in-vivo* studies compatible with the short half life of Tc99m. (Fig 6,7)

Developed methods to radiolabel polymer nanoparticles

**Propose:** To develop a radio-labeling method for PLGA NPs with Tc99m for biodistribution studies.
**Scope:** We conjugated Tc99m to BSA, and encapsulated the complex into the NPs. Use of chelating agents recommended on the initial proposal were unsuccessful.
**Major findings:** The conjugate was stable *in-vitro* and *in-vivo*; with good labeling efficiency and the total label was compatible with *in-vivo* studies. Previous attempts included Tc99 conjugation to chelating agents; both of these were incompatible with NP preparations. (Fig 6,7)

Successfully transferred our nanoparticle preparation protocols; Started *in-vivo* biodistribution

**Propose:** To prepare Tc99m labeled NP at the place of the animal studies (UTHSCSA labs of Radiology).
**Scope:** To set up equipment and procedures at the site of animal studies and to test drive the techniques.
**Major findings:** We were able to reproduce the procedures and to generate materials for animal testing with specific activity compatible with *in-vivo* studies.

Developed alternate procedures for preparing nanoparticles)

**Propose:** To explore alternate NP fabrication procedures that will allow efficient Tc99m labeling and prolonged *in-vivo* blood levels.
**Scope:** We tested several procedures for Tc99m NP fabrication. Selected procedures from recent literature were based on claims of prolonged blood circulation levels. The goal was to keep the NP as the main technology, avoiding major changes such as liposome formulations, but at the same time, exploring minor modifications to prolong blood circulation time *in-vivo*.
**Major findings:** None of the alternative procedures were with compatible with Tc99m tracer. Particle size from alternative procedures were larger than 200nm and this effort was abandoned.

Synthesized and fully characterize PLA-b-PEG-Maleimide block Polymer (PLA-b-PEG-MAL)

**Propose:** To synthesize Maleimide modified PLGA-b-PEG 2000 for NPs bone-targeted formulations. (This material is not commercially available)
**Scope:** Using ring opening reaction, synthesize PLA-b-PEG-MAL.
**Major findings:** This polymer was synthesized and characterized by H-NMR. (Appendix 2)

Improved lyostability of polymer nanoparticles, with and without PEG modification

**Propose:** To develop methods for long term storage of NPs.
**Scope:** Test different surfactant at range of concentrations for effect on particle size and charge after freeze drying.
**Major findings:** F68, a commonly used cryo-preserative was shown to be effective in maintaining particle size when used at 100 fold excess over NP content. The common sugar sucrose was also effective. Data for sucrose was given in previous reports. (Fig 1-5)

Encapsulated two proteasome inhibitors, and determined their *in-vitro* release profiles

**Propose:** To demonstrate the encapsulation and release profile of proteasome inhibitors.
**Scope:** Standard procedures were used for efficient drug loading into targeted and non-targeted NPs, drug loading and release was measured using simple UV absorbance.
**Major findings:** Velcade, a model and the only FDA approved proteasome inhibitor, was encapsulated in an NP. These released NPs released close to 80% in 24 hours period. (Fig 12, 13)

Developed proteasome activity assay to determine activity of encapsulated drug

**Propose:** To demonstrate the activity of proteasome inhibitor (Velcade) before and after NP drug encapsulation.
**Scope:** Use cell based assay (5TGM1 myeloma cells) to measure *in-vitro* activity of compounds before and after encapsulation.
**Major findings:** Activity of Velcade was the same before and after encapsulation. (Fig 11)

Developed *in-vitro* assay to determine affinity of bone-targeting nanoparticles

**Propose:** To demonstrate *in-vitro* binding using bone-equivalent materials.
**Scope:** Hydroxyapatite materials were tested for NPs binding with two ligand and with two tracers.
**Major findings:** *In-vitro* binding was demonstrated. Background and non-specific binding are significant. (Fig 9, 10)

.

# Table of Contents


1. **Introduction** ..... 3
2. **Body** ..... 4
3. **Key Research Accomplishments** ..... 32
4. **Reportable Outcomes** ..... 34
5. **Conclusions** ..... 36
6. **References** ..... 36
7. **Appendices** ..... 37

## 1. Introduction

The goal of this project was to determine, in preclinical studies, the potential of skeletally targeted polymeric nanoparticles as carriers of the proteasome inhibitor Bortezomib (Velcade), to be used as a selective and efficacious treatment of Multiple Myeloma.

In clinical oncology practice, Velcade is a chemotherapeutic agent currently approved for the treatment of myeloma in the relapsed setting post transplant or as a second line treatment in patients unsuitable for transplantation. In a clinical trial, Velcade patients had a significantly higher rate of overall survival (80 per cent) versus patients who received dexamethasone alone. However, Velcade causes significant problems including systemic toxicity, which limits the actual therapeutic window and efficacy of the treatment. Our hypothesis is that bone-targeting nanocarriers can preferentially accumulate in the skeleton and locally release Velcade to impair the capacity of myeloma cells to survive and grow *in vivo,* thereby reducing the formation and growth of tumor-induced lytic bone lesions. Otherwise, Velcade is not selective to bone.

The major tasks of this research were:

1) Formulate and characterize drug-containing, bone-targeting nanoparticles.
2) Determine the *in vivo* biodistribution of bone-targeting nanoparticles.
3) Evaluate the efficacy of bone-targeted delivery of proteasome inhibitors on myeloma tumor progression using the well-characterized 5TGM1 GFP label murine model of myeloma.

Under this grant, we have demonstrated the preferential biodistribution of nanoparticles specifically designed to target and adhere to bone matrices. We have shown that these same nanoparticles can selectively deliver Velcade to skeletal sites to act as an anti-myeloma agent. Targeted bone delivery has several potential benefits, including reduced systemic exposure, increased efficacy in the targeted microenvironment, and the ultimate opportunity to reverse catastrophic disease processes. Furthermore, targeted delivery to bone has several additional significant application opportunities in the areas of bone metastasis, osteoporosis, fracture healing, cartilage repair, and tissue engineering.

This final report contains previous key information presented as graphs and tables demonstrating work achieved on formulation and in preliminary biodistribution studies. The second part of the report contains the latest biodistribution results presented as unprocessed data and graphs for easy visualization of the results. This new information is under the title “Biodistribution studies”.

Task 3 consisted of testing the efficacy of formulated nanoparticles using an *in vivo* model of multiple myeloma. This task was delayed until very recently because of an animal shortage and unconfirmed dates for delivery. This situation was beyond the control of the investigators and the army grant manager was notified during our communications. The solution to the problem was found when our collaborator at UTHSCSA suggested the use of alternative species. This solution was immediately adopted and is in progress as we prepare this final report.

## 2. Body

The project is broken down into the following tasks:

1) Formulation and characterization of drug-containing, bone-targeting nanocarriers.
2) Determination of the *in vivo* biodistribution of bone-targeting nanocarriers.
3) Demonstration of the efficacy of bone-targeted delivery of proteasome inhibitors on myeloma tumor progress.

Task 1 was scheduled to occur during years 1 and 2.
Task 2 was scheduled to occur during years 2 and 3 with some overlap with Task 1.
Task 3 was scheduled to occur during the last year and half of the project.

This final report is a compilation of the most relevant data collected and previously reported; the data presented was selected to address the tasks listed above. This report also includes new data on work performed since our last report, and completes the extensive work on biodistribution. Task 3, which deals with the efficacy of the formulated nanoparticles, was just recently initiated and is in progress. No task 3 data has been included in this final report and will be provided as an amendment when results are available (Final efficacy report it is been prepared by Professor Babatunde O. Oyajobi at UTHSCSA).

1) Task 1 is focused on the development of the bone-targeting nanoparticles and is broken down into the following subtasks:

- Selection of proteasome inhibitors for *in vivo* studies. Completed and reported in the first annual report.
- Formulation and characterization of bone-targeting nanoparticles. Completed and discussed in the first and second annual reports.
- Demonstration of adhesion of bone-targeting nanoparticles to bone-like substrates *in vitro*. Completed and discussed in the second and third annual reports.
- Formulation of proteasome inhibitors into bone-targeting nanoparticles. Completed and discussed in the second annual report.

### 2.1 Formulation of Nanoparticles

Nanoparticles were prepared by a water-and-oil emulsification method, followed by solvent evaporation. Figures 1 and 2 show the characterization of particle size as a function of polymer concentration and as a function of PEG concentration, respectively. These figures show that as the PLGA polymer solution concentration is decreased (diluted), the nanoparticle size decreases. Also, as the PEG concentration increases, the nanoparticle size decreases.

Results on surface charge characterization (Zeta potential) as a function of PEG concentration are shown in Figure 3: the higher the PEG content, the more neutral are the nanoparticles, as determined in a phosphate buffer solution. Particles made with 100% PLGA-PEG are almost neutral. Figure 4 shows an E-SEM microphotograph to confirm the particle size. Finally, Figure 5 shows the effect of the cryo-protectant Pluronic F68 mixed at different ratios to avoid particle agglomeration during the freeze drying process. As shown in Figure 5, the size (nm) is represented as a function of the ratio of cryo-protecting agent (F-68) to PLA-PEG.

**Figure 1:** Nanoparticles size as a function of polymer concentration

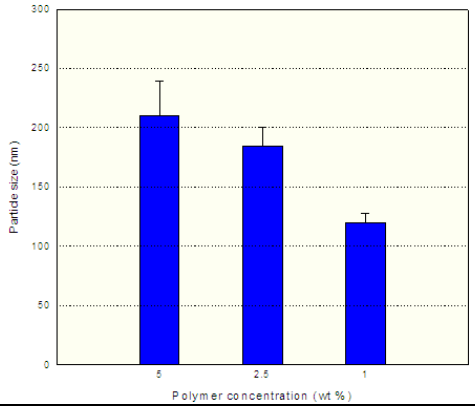


**Figure 2:** Nanoparticle size as a function of PEG concentration

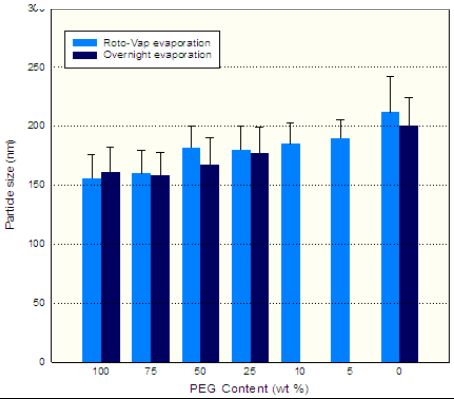


**Figure 3:** Zeta potential as a function of PEG concentration

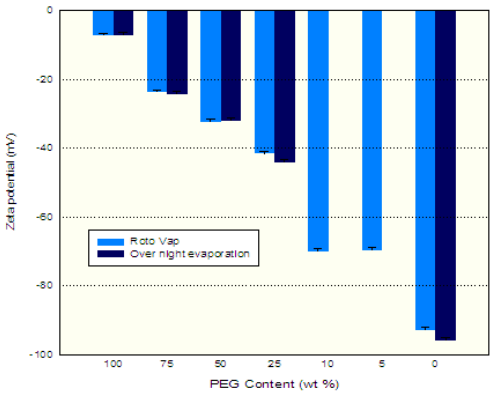


**Figure 4:** SEM picture (scanning electron micrograph)

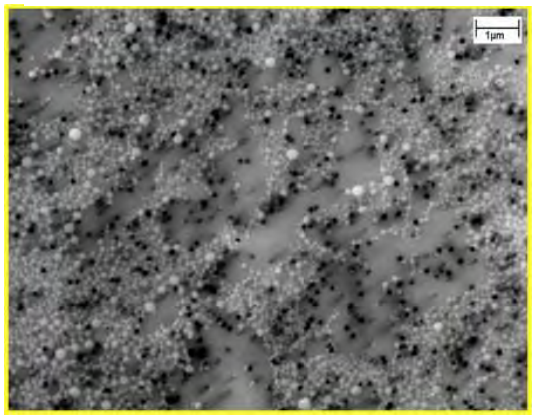


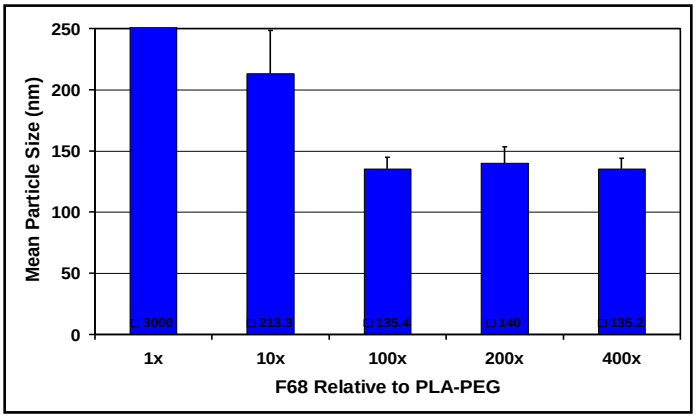


**Figure 5:** Nanoparticle size after freeze drying as a function of F68 to PLA-PEG ratio (cryo-preservation agent)

$^{99m}$Tc Radiolabeling of Nanoparticles

We developed unique radio-labeling protocols using a multi-variable approach that included reducing labeling time, decreasing particle size, increasing PEG content, and reducing surface charge. All of these strategies were investigated and optimized to generate better material for the *in vivo* animal studies.

Our initial approach was to develop methods of radio-labeling nanoparticles in preparation for biodistribution studies planned in Task 2. We selected the gamma emitter $^{99m}$Tc, with a 6.5 hr half-life, based on the experience of our collaborators at The University of Texas Health Science Center at San Antonio (UTHSCSA). $^{99m}$Tc is hydrophilic and provided as an aqueous solution from the cyclotron source. We originally proposed chelating this radionuclide with a lipophilic chelator HMPAO or others, mirroring methods to label liposomes, and to facilitate encapsulation using our simple precipitation protocol. However, this approach was not successful. After examining several commercial chelators, we found that both the chelation and the encapsulation efficiency were very dependent on the 'quality' of the radionuclide. $^{99m}$Tc is subject to oxidation, which affects chelation efficiency and, in turn, affects encapsulation efficiency. In most cases, encapsulation efficiency was less than 20%, which was deemed as insufficient. Subsequently, we explored the conjugation of $^{99m}$Tc to reduced proteins, such as bovine serum albumin (BSA), to improve its loading efficiency into nanoparticles (Figure 6). This yielded encapsulation efficiencies of 90% or greater. Payload stability was monitored over a 24-hour period and was found to be nearly 100%. Figure 7 shows *in vitro* stability in serum and in PBS, and Figure 8 demonstrates *in vivo* stability of non-targeted nanoparticles (in this case, most of the label was found in the liver with a very small amount seen in the bladder, the bladder fraction representing free $^{99m}$Tc *in vivo*).

However, we had concerns related to residual reducing agent. This agent was used to activate the protein and can cause interference with the coupling of bone-targeting ligands to functionalized nanoparticles. Therefore, we modified the radio-labeling method to use a commercial reducing gel that can be removed from the protein preparation by simple centrifugation. The newly reduced, clean protein can then be used to complex the radionuclide for encapsulation using the same procedure described previously. The encapsulation efficiency was unaffected by this slightly altered approach. Furthermore, this modified method avoided a lengthy column separation process that diminished the amount of available radioactivity (yield).

**Figure 6:** Radiolabeling of nanoparticles using oxidized, fresh or conjugated $^{99}$Tc into BSA

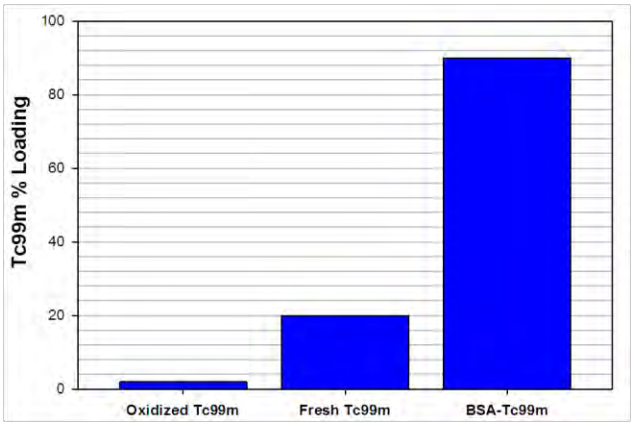


**Figure7:** Relative stability of $^{99m}$Tc label nanoparticles in vitro after 24 hours incubation

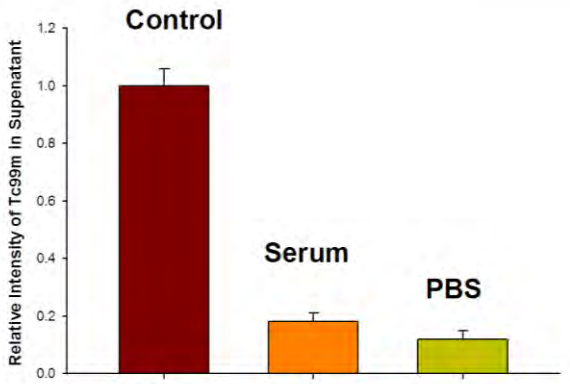


**Figure 8:** Stability of $^{99m}$Tc nanoparticles in vivo measured by SPECT technique at 2 hours post-injection

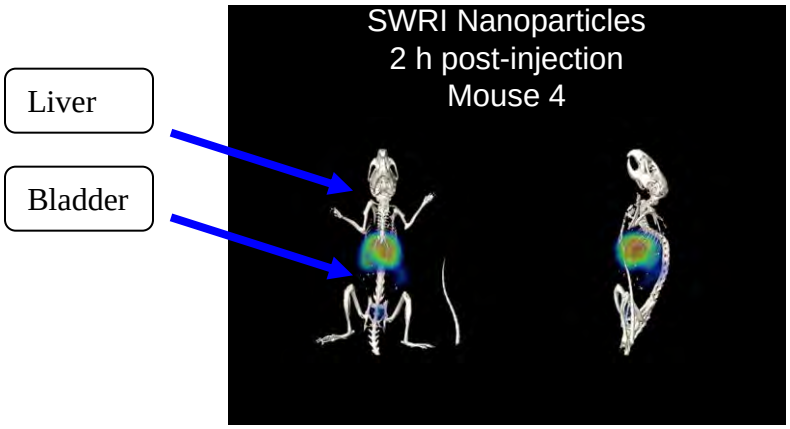


## 2.2 Ligand Quantification

After testing different unsuccessful methods for direct ligand quantification, we developed our own procedure to quantify the ligand content directly. The method used acid hydrolysis and colorimetric absorbance detection; a method similar to the one used for amino acid analysis. On previous attempts, we had tried Nuclear Magnetic Resonance (NMR) techniques to quantify the ligand. In retrospect, the size of the polymer relative to the small size of the ligand made this approach very difficult.

Acid hydrolysis of the conjugated ligand was followed by primary amine detection with OPA reagent (O-Phtalaldehyde) (See Appendix 3). In this method, nanoparticles were treated by controlled acid hydrolysis. This is a procedure similar to amino acid analysis of proteins. The released amino ligand was quantified using a sensitive fluorescent amino terminus reagent (OPA).

To test this method, we made nanoparticles and conjugated the ligand on the surface using maleimide chemistry or made nanoparticles using our custom made polymer, which was already conjugated with the targeting ligand before nanoparticle formation (PLGA-PEG-LIGAND).

Using this procedure, we were able to detect the presence of the ligand in all of the targeting polymers synthesized so far. We found that the conjugation efficiency was a variable that depended on the route of synthesis. It varied from 5% for the ASP4 ligand to 25% efficiency for the BP ligand. This method is now a standard technique for ligand quantification.

### **2.3** Hydroxyapatite Binding (HAp Binding)

As a first approach, (Method #1) we created ligand-nanoparticle containing functionalized surfaces (Maleimide reactivity) followed by conjugation with targeting ligand. After a cleanup procedure (centrifugation step) to remove the free ligand, the nanoparticles were tested for HAp binding. To improve the sensitivity of this technique, radio-labeled nanoparticles were used.

As a second approach, (Method #2) nanoparticles made with polymers already containing ligands (PLGA-PEG-BP and PLGA-PEG-ASP4) blended with different ratios of PLGA-PEG. The resulting nanoparticles were used to evaluate HAp *in vitro* binding. This approach was developed using the successful synthesis of the starting materials discussed below (see synthesis Appendix 2).

However, the binding experiments performed with NP construct made via this approach were unsuccessful. It is possible that the ligand exposure using pre-conjugated polymers is much lower than when using post conjugation of pre-made nanoparticles. Figure 9 and Figure 10 show *in vitro* binding data using post conjugation methods (particles fabricated with PLGA-PEG-MAL; ligand is conjugated onto their surfaces afterward). The reactivity of maleimide (MAL) is used post particle formation to conjugate the targeting ligand. This approach seems to be working and is the method used for all of the *in vitro and in vivo* studies, as shown below. Figure 9 shows binding to HA using a bisphosphonate (BP) or poly aspartic acid (ASP6). $^{99m}$Tc labeling was used as a tracer. Figure 10 shows HA binding results for the ASP6 ligand using a dye as a tracer. The two methods demonstrate specific binding with some small amount of background binding. The background binding can be due to the entrapment of nanoparticles within HA micro-particles.

It is important to mention that pre-made polymers with ligand included in the starting materials (PLGA-PEG-Ligand) could in theory simplify the development of this technology. This was contemplated in the initial proposal. However, this approach has been more difficult than anticipated. Alternatively, this approach could also produce unexpected results such as reduced efficacy seen by us.

**Figure 9.** *In vitro* nanoparticle binding for two different ligands (BP and ASP6 polymeric form of aspartic acid).

Bisphosphonate (BP) Poly Aspartic acid (ASP6)

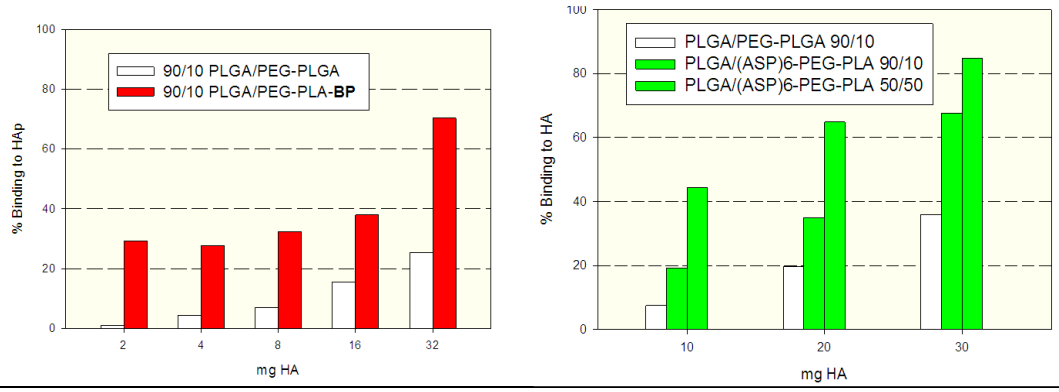


**Figure 10:** Hydroxyapatite binding using a dye as a tracer, (there is a small (~5%) binding of the non-targeted control).

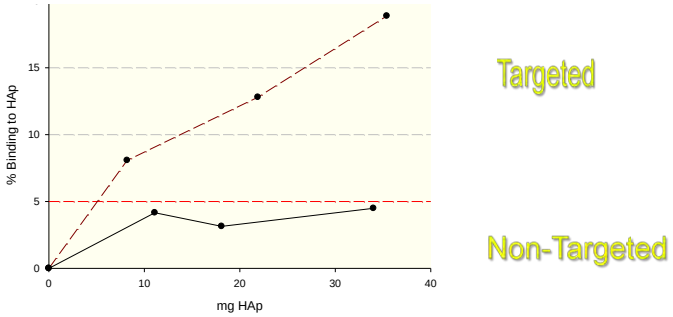


## 2.4 Synthesis

PLGA-PEG-BP and PLGA-PEG-ASP4 polymers were synthesized, and we were able to produce the final materials at 5-25% yield quantified using the OPA technique (see appendix 3). To improve the yield, we developed alternative routes that resulted in even higher yield of the final product. This material was tested multiple times but it was less effective or just ineffective in terms of producing nanoparticles with binding affinity for bone substitutes. Therefore this approach was abandoned. All our *in vivo* studies were performed using the post particle conjugation strategy (Method #1 in page 8)

Cell Based Testing of Velcade-Loaded Nanoparticles

For our cell based study, we used the FDA approved drug, Velcade TM. This drug was loaded in nanoparticles and tested *in vitro* using the 5TMG1-GFP myeloma cell line. This cell line was obtained from our collaboration with Dr. Greg Mundy's lab at Vanderbilt University in Nashville, Tennessee, and is the same cell line used in our efficacy studies. The results indicated that Velcade remains active after

encapsulation (Figure 11). Controlled drug release is shown in Figure 12 and Figure 13 represented as total and cumulative drug release. A 100% release was demonstrated after a 7 day period.

**Figure 11:** Cytotoxicity of Velcade (Bortezomib) free drug or nanoparticle loaded drug on 5TMG1 Myeloma cells line after 24 hours treatment. (Activity measured with MTT assay)

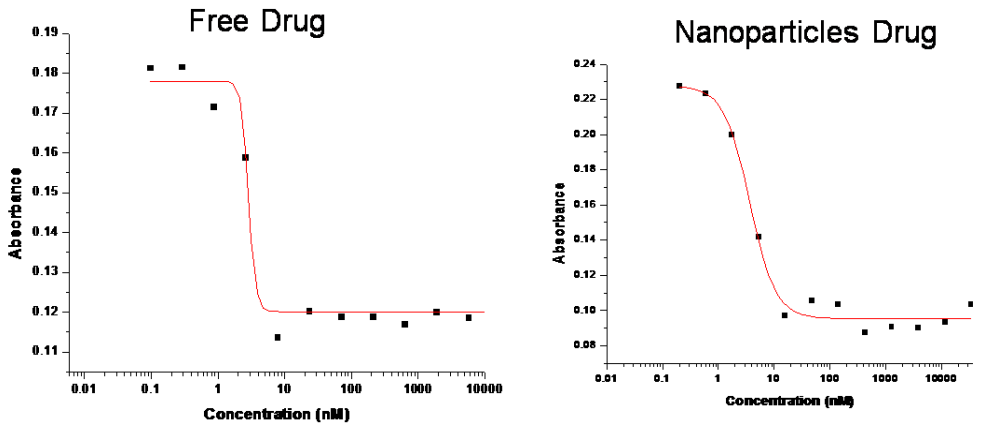


**Figure 12:** Drug release from nanoparticles (Velcade) in phosphate buffer expressed as µg/ml of drug released

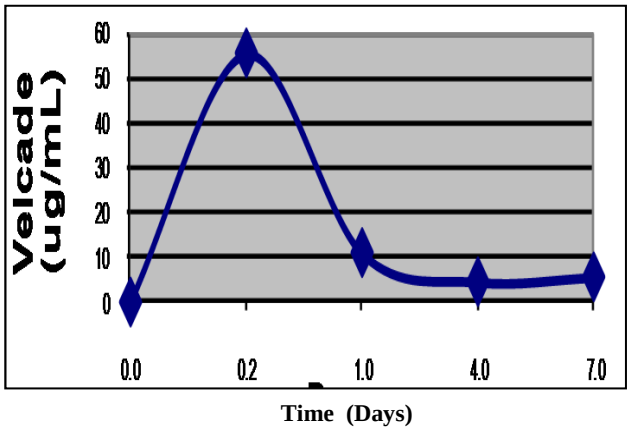

**Figure 13:** Drug release from nanoparticles (Velcade) in phosphate buffer expressed as cumulative percentage of drug released

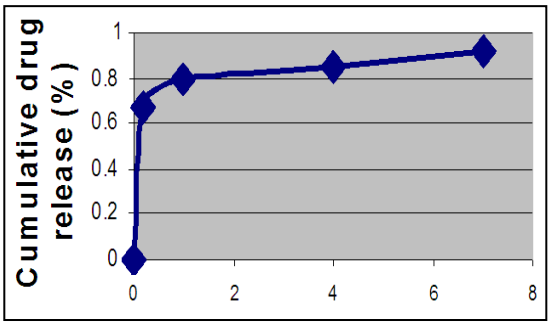


Notes:

Velcade: Recommended clinical dose = 1.3 mg/m$^2$.
Rat equivalent = 0.2 mg/kg in rat

Drug loading: 0.1-1.5% (5-15 µg/mg) for tested formula
Nanoparticles usage: typical 2mL/kg injection at 10mg/mL concentration can reach the require dosage in animals

2) Task 2 concerned with the assessment of the *in vivo* biodistribution of bone-targeting nanoparticles in a myeloma mouse model. The task is broken down into the following subtasks:

- Preparation of radio-labeled bone-targeting nanoparticles.
- *In vivo* biodistribution assay.

Both of these tasks were completed.

We conducted initial animal trials in late November/early December 2007, which allowed us to confirm our *in vivo* protocols and test initial nanoparticle formulations. Particle formulations and radiolabel content were more than sufficient to permit *in vivo* imaging; the initial particle size was 180 nm and proved too large to support long-term distribution. This led to further development to reduce the particle size, which raised some previously unknown issues with nanoparticle formulation by-products on smaller nanoparticle colloidal stability. This forced us to resolve these issues before proceeding with additional *in vivo* studies. We performed the final *in vivo* biodistribution study in April 2010.

The figures below present the key results of the initial exploratory biodistribution studies. These studies were done using 120 nm and 200 nm nanoparticles and non-diseased mice. Biodistribution studies were performed on 6 animals per group; freshly made nanoparticles loaded with $^{99m}$Tc were injected in mice

by tail vein injection. Figure 14 shows selected bone biodistribution after 24 hours, Figure 15 shows biodistribution to selected tissues after 24 hours and Figure 16 shows blood clearance from 0-44 hours. Bars in Figures 13-15 represent mean ±SD (n=6).

**Figure 14:** Bone biodistribution of two particle sizes (120 and 200 nm) at 24 hr

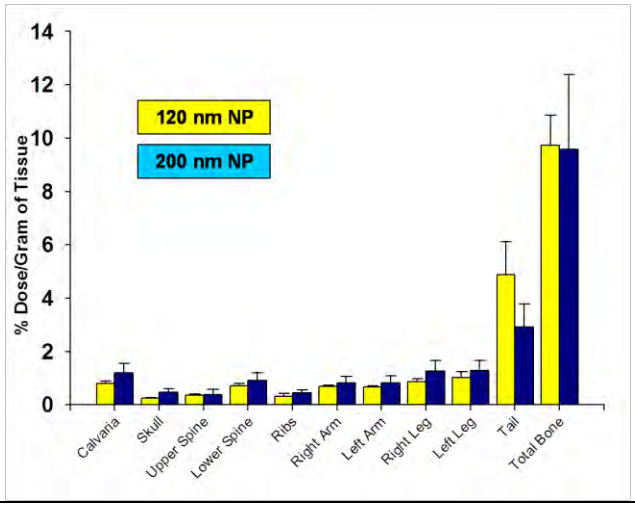


**Figure 15:** Whole body biodistribution at 24 hr.

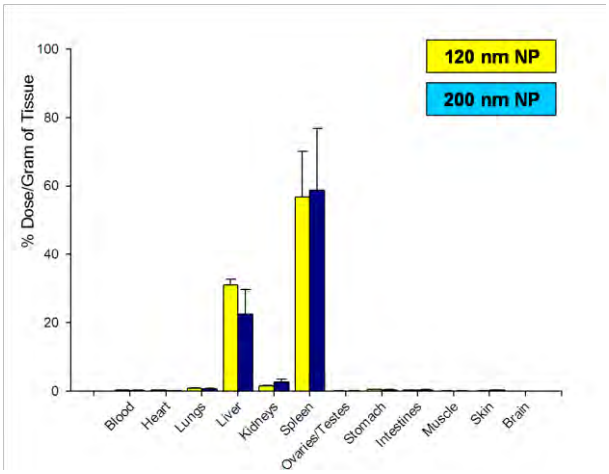

**Figure 16:** Blood levels for two particle sizes 0-44 hr.

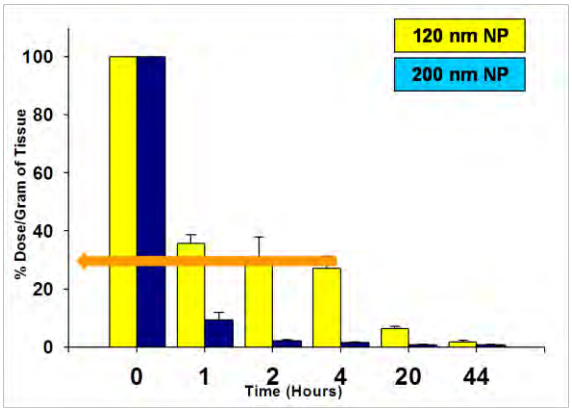


Because of the reduced blood circulation time on the initial experiments, we investigated procedures to modify the nanoparticle formulation methods using the optimized radio-labeling techniques developed after the first pilot biodistribution study. Compared with the above results, we observe now a prolonged half-life for the non-targeted nanoparticles. However, the targeted nanoparticles had a reduced time in blood and were removed from circulation at the same rate as before. This is probably due to the surface modification introduced with the targeting ligand. An alternative explanation is that more nanoparticles are taken by bone and removed from circulation, but this was not demonstrated by quantification of bone uptake.

The figures below show biodistribution performed on 6 animals per group; freshly made nanoparticles of about 100nm size, and loaded with $^{99m}$Tc were injected in mice by tail vein injection. Figure 17 shows blood levels of targeted nanoparticles. Figure 18 shows blood levels of non targeted nanoparticles. Figure 19 shows bone distribution of non-targeted and targeted nanoparticles. Bars in Figures 17-19 represent mean ± SEM (n=6).

As seen in figure 16, 120nm NPs have a longer circulation time in blood, versus 200nm that are removed from the blood as quickly as 1 hour after tail vain injection. This has been reported before with slightly different formulations, but was confirmed to make sure we have sufficient circulation time for bone-targeting using our formulations.

To compare the circulation times of targeted and non-targeted NPs, we performed *in-vivo* testing (seen in figure 17, 18). Figure 18 shows a prolonged blood circulation of non-targeted NPs, which is better than the circulation times shown in figure 16. This was attributed to our improved techniques and experience on the NPs formulation. However, targeted NPs have a reduced circulation time in blood as compared to same NPs (120nm) in figure 16 independent of the disease status. This was attributed to filtration of targeted particles, and organs such as the spleen and liver where most of the Tc99m was found.

Figure 19, shows bone biodistribution of NPs. There is a small background accumulation of targeted and non-targeted NPs in bone (~2% of total dose) and a differential accumulation of targeted NPs that is higher in Myeloma mice than control animals (6% for targeted versus 3% for non-targeted NPs). This 3%

differential was encouraging and the positive result of this study is knowing that most of the targeted NPs are removed in the liver or spleen.

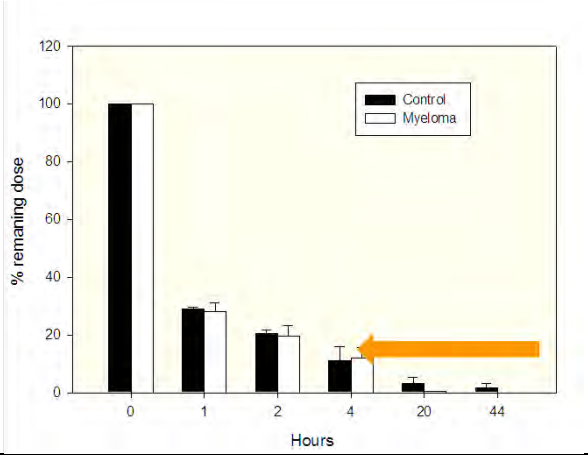


**Figure 17:** *In vivo* blood biodistribution in mice (n=6)

Targeted

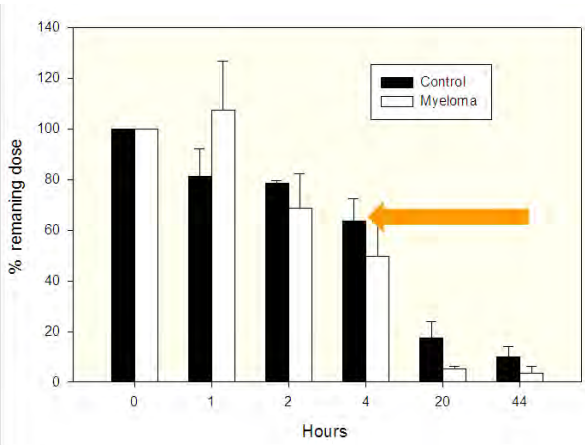


**Figure 18:** *In vivo* blood biodistribution in mice (n=6)

Non-Targeted

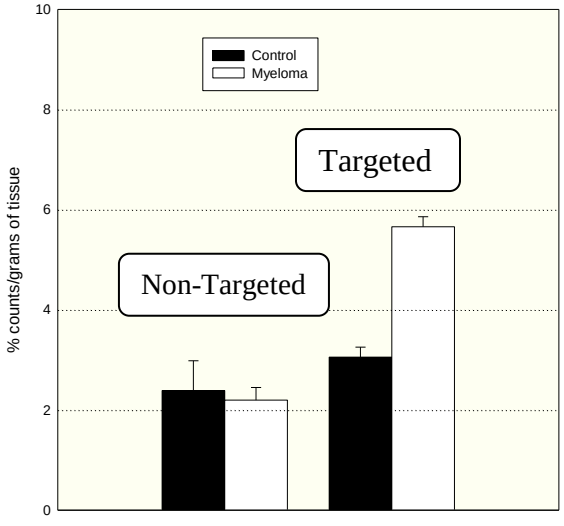


**Figure 19:** Bone biodistribution in mice (n=6)

**2.5** Final biodistribution study

In April of this year, we conducted a final biodistribution study using normal and tumor bearing mice. Our goal was to fine-tune the amount of PEG coating to prolong systemic circulation. We tested a 5% and a 15% PEG loading (5% or 15% by weight PEG expressed as a percentage of the PLGA-PEG total polymer). All of the formulations were $^{99m}$Tc loaded without Velcade, and the groups tested are shown on the table below. The intended animal group size was 7 animals for tumor bearing mice and 3 for control mice; however we lost some animals on the control groups during the study due to the actual nanoparticle injections (see table below).

Table 1: Nanoparticles formulations tested for biodistribution

| Date | Formulation | Intended mice groups | Actual mice groups |
|---|---|---|---|
| 3-25-2010 | 5% PEG Non Targeted | Tumor n=7 control n=3 | Tumor n=7 control n=3 |
| 3-26-2010 | 15% PEG Non Targeted | Tumor n=7 control n=3 | Tumor n=7 control n=3 |
| 3-29-2010 | 5% PEG Targeted | Tumor n=7 control n=3 | Tumor n=7 control n=2 |
| 4-5-2010 | 15% PEG Targeted | Tumor n=7 control n=3 | Tumor n=7 control n=0 |

We tested four $^{99m}$Tc nanoparticle formulations in green fluorescent protein (GFP) tumor-bearing and control mice. Each conscious mouse was injected with 0.1 mL (~0.5 mCi per mouse) $^{99m}$Tc nanoparticle formulation in the tail vein using a syringe with a 27½ gauge needle. Immediately following injection, the mice were anesthetized by inhalation of 2% isoflurane in 100% oxygen and blood was collected into VWR heparinized hematocrit tubes from retro-orbital sinus.

The clearance of the $^{99m}$Tc-nanoparticles from the blood (Table 2 and Table 3) was determined by counting blood samples collected at various times post-injection. For each formulation there does not appear to be big differences in clearance kinetics between tumor-bearing and control mice. The 3-25-2010 batch cleared from circulation faster than the other formulations tested. The formulations on 3-26-2010 and 3-29-2010 had similar clearance kinetics which remained slightly longer in circulation than the 3-25-2010 formulation. The 4-5-2010 formulation remained in circulation for a prolonged time compared with the other formulations. For each formulation, a large percentage of the $^{99m}$Tc nanoparticles were removed from circulation within the first four hours into mainly the liver and spleen.

Table 2: Normalized % $^{99m}$Tc Activity in Blood; Mean (SEM)

| Time (h) | | | | |
|---|---|---|---|---|
| | 3-25-2010 Unconjugated Tumor | 3-25-2010 Unconjugated Control | 3-26-2010 Unconjugated PEG Tumor | 3-26-2010 Unconjugated PEG Control |
| 0 | 100 (0) | 100 (0) | 100 (0) | 100 (0) |
| 1 | 18.72 (3.17) | 18.24 (4.93) | 28.42 (5.19) | 28.69 (12.99) |
| 2 | 14.69 (2.20) | 17.72 (5.45) | 23.77 (4.17) | 22.05 (9.70) |
| 4 | 8.96 (1.56) | 14.00 (5.08) | 17.18 (3.10) | 17.79 (6.85) |
| 20 | 0.59 (0.18) | 2.14 (1.80) | 4.46 (1.03) | 5.09 (2.47) |
| 44 | 0.21 (0.05) | 1.97 (1..94) | 0.04 (0.01) | 0.09 (0.07) |

Table 3: Normalized % $^{99m}$Tc Activity in Blood; Mean (SEM)

| Time (h) | | | | |
|---|---|---|---|---|
| | 3-29-2010 Targeted Tumor | 3-29-2010 Targeted Control | 4-5-2010 Targeted PEG Tumor | 4-5-2010 Targeted PEG Control |
| 0 | 100 (0) | 100 (0) | 100 (0) | 100 (0) |
| 1 | 26.53 (3.25) | 16.36 (1.03) | 54.16 (8.36) | 50.49 |
| 2 | 18.11 (2.14) | 13.14 (0.87) | 46.68 (8.21) | 37.52 |
| 4 | 12.22 (1.07) | 11.63 (0.66) | 41.29 (5.94) | 35.08 |
| 20 | 0.84 (0.27) | 0.32 (0.06) | 10.64 (2.35) | 6.99 |
| 44 | 0.04 (0.01) | 0.02 (0.00) | 0.15 90.05) | 0.07 |

At 44 h post-injection and immediately after the imaging session, blood was collected by cardiac puncture in the anesthetized mice. The mice were then euthanized by cervical dislocation. Tissues were collected in 10% formalin and selected bones were collected in paraformaldehyde for GFP optical imaging. Tissues were removed from the bones prior to fixation. Samples were weighed and counted, and organ distributions calculated. The % ID per organ for non-bone organs are shown in table 4 and 5 below. For all groups, the liver and spleen had the most uptake of the non-bone organs. In some animals, we noted large ovaries and uptake in these tissues.

Table 4: Total body tissue distribution expressed as percent of injected dose per total organ

| Organ | % ID/ organ 3-25-2010 Unconjugated Tumor Mean (SEM) | % ID/ organ 3-25-2010 Unconjugated Control Mean (SEM) | % ID/ organ 3-26-2010 PEG Tumor Mean (SEM) | % ID/organ 3-26-2010 PEG Control Mean (SEM) |
|---|---|---|---|---|
| Blood | 0.265 (0.101) | 0.101 (0.040) | 0.143 (0.045) | 0.136 (0.018) |
| Heart | 5.533 (6.492) | 0.011 (0.007) | 0.043 (0.010) | 0.021 (0.006) |
| Lungs | 0.370 (0.065) | 0.198(0.097) | 0.178(0.026) | 0.121(0.029) |
| Liver | 30.326 (5.052) | 25.391(11.786) | 27.823(6.927) | 35.314(7.151) |
| Kidneys | 0.451 (0.149) | 0.386 (0.073) | 0.381(0.065) | 0.443(0.047) |
| Spleen | 8.667 (1.583) | 9.982 (4.751) | 2.736(0.583) | 3.370(0.931) |
| Ovaries/Testes | 0.167 (0.106) | 0.083 (0.036) | 0.128(0.044) | 0.124(0.023) |
| Stomach | 0.185 (0.090) | 0.095(0.031) | 0.153(0.028) | 0.109(0.019) |
| Intestines | 0.423 (0.189) | 0.502(0.064) | 0.826(0.079) | 0.983(0.165) |
| Muscle | 1.003 (0.795) | -6.779 (6.884) | 1.045(0.271) | 1.104(0.878) |
| Skin | 0.382 (0.147) | 0.267 (0.050) | 0.687(0.136) | 0.713(0.109) |
| Brain | 0.067 (0.046) | -0.003 (0.001) | -0.001(0.001) | 0.000(0.003) |

Table 5: Total body tissue distribution expressed as percent of injected dose per total organ

| Organ | % ID/ organ 3-29-2010 Targeted Tumor Mean (SEM) | % ID/ organ 3-29-2010 Targeted Control Mean (SEM) | % ID/ organ 4-5-2010 Targeted PEG Tumor Mean (SEM) | % ID/ organ 4-5-2010 Targeted PEG Control Mean |
|---|---|---|---|---|
| Blood | 0.099 (0.023) | 0.099 (0.031) | 0.064(0.023) | 0.102 |
| Heart | 0.019 (0.004) | 0.014 (0.000) | 0.015(0.004) | 0.019 |
| Lungs | 0.130 (0.025) | 0.196 (0.116) | 0.139(0.073) | 0.089 |
| Liver | 38.149 (6.941) | 49.612 (0.252) | 13.663(4.294) | 26.429 |
| Kidneys | 0.325 (0.030) | 0.386 (0.012) | 0.224(0.035) | 0.310 |
| Spleen | 5.370 (1.076) | 6.465 (0.476) | 1.349(0.362) | 2.396 |
| Ovaries/Testes | 0.069 (0.038) | 0.040 (0.006) | 0.033(0.013) | 0.021 |
| Stomach | 0.122 (0.012) | 0.093 (0.023) | 0.081(0.039) | 0.059 |
| Intestines | 0.568 (0.050) | 0.586 (0.027) | 0.538(0.123) | 1.194 |
| Muscle | 0.130 (0.051) | 0.328 (0.302) | -0.008(0.047) | 0.034 |
| Skin | 0.375 (0.061) | 0.620 (0.028) | 0.290(0.060) | 0.680 |
| Brain | 0.000 (0.001) | -0.005 (0.000) | -0.001(0.004) | 0.021 |

The following tables (6 and 7) show the biodistribution data of non-bone tissues calculated as % ID/g tissue.

Table 6: Total body tissue distribution expressed as percent of injected dose per gram of tissue

| Organ | % ID/ g 3-25-2010 Unconjugated Tumor Mean (SEM) | % ID/ g 3-25-2010 Unconjugated Control Mean (SEM) | % ID/ g 3-26-2010 PEG Tumor Mean (SEM) | % ID/g 3-26-2010 PEG Control Mean (SEM) |
|---|---|---|---|---|
| Blood | 0.232(0.090) | 0.094(0.041) | 0.132(0.0400 | 0.122(0.014) |
| Heart | 47.272(55.494) | 0.100(0.065) | 0.438(0.137) | 0.224(0.065) |
| Lungs | 2.201(0.411) | 1.060(0.518) | 1.129(0.225) | 0.682(0.158) |
| Liver | 27.037(4.152) | 23.348(10.920) | 27.878(6.867) | 35.492(6.221) |
| Kidneys | 1.320(0.388) | 1.236(0.246) | 1.402(0.229) | 1.629(0.108) |
| Spleen | 104.663(21.620) | 141.846(74.725) | 33.285(9.707) | 58.761(12.759) |
| Ovaries/Testes | 5.629(4.314) | 0.252(0.164) | 0.502(0.201) | 12.357(12.107) |
| Stomach | 0.431(0.198) | 0.332(0.137) | 0.307(0.046) | 0.339(0.028) |
| Intestines | 0.175(0.074) | 0.251(0.040) | 0.385(0.036) | 0.465(0.049) |
| Muscle | 0.113(0.086) | -0.844(0.858) | 0.138(0.035) | 0.146(0.118) |
| Skin | 0.152(0.061) | 0.107(0.022) | 0.277(0.053) | 0.277(0.037) |
| Brain | -0.816(1.235) | -0.007(0.004) | -0.002(0.002) | -0.002(0.009) |

Table 7: Total body tissue distribution expressed as percent of injected dose per gram of tissue

| Organ | % ID/ g<br>3-29-2010<br>Targeted<br>Tumor<br>Mean (SEM) | % ID/ g<br>3-29-2010<br>Targeted<br>Control<br>Mean (SEM) | % ID/ g<br>4-5-2010<br>Targeted PEG<br>Tumor<br>Mean (SEM) | % ID/g<br>4-5-2010<br>Targeted PEG<br>Control<br>Mean |
|---|---|---|---|---|
| Blood | 0.089(0.021) | 0.086(0.027) | 0.059(0.021) | 0.081 |
| Heart | 0.165(0.031) | 0.136(0.011) | 0.206(0.059) | 0.334 |
| Lungs | 0.698(0.163) | 1.347(0.985) | 0.784(0.423) | 0.524 |
| Liver | 33.897(5.887) | 47.669(4.782) | 13.582(4.376) | 28.357 |
| Kidneys | 1.162(0.107) | -4.095(5.673) | 0.903(0.163) | 1.493 |
| Spleen | 57.119(12.506) | 64.566(14.931) | 21.371(9.472) | 36.310 |
| Ovaries/Testes | 14.023(13.940) | 0.138(0.036) | 10.893(4.291) | 7.161 |
| Stomach | 0.271(0.037) | 0.292(0.114) | 0.213(0.089) | 0.271 |
| Intestines | 0.248(0.020) | 0.256(0.007) | 0.298(0.099) | 0.876 |
| Muscle | 0.016(0.006) | 0.040(0.045) | -0.001(0.006) | 0.004 |
| Skin | 0.147(0.024) | 0.235(0.012) | 0.117(0.025) | 0.236 |
| Brain | -0.001(0.003) | -0.012(0.002) | -0.003(0.009) | 0.047 |

The biodistribution data of the % injected dose (ID) per organ for the various bones and total bone are shown below (tables 8 and 9). In certain animals, the $^{99m}$Tc nanoparticles infiltrated in the tail upon injection, so this needed to be taken into account when comparing the bone uptake values.

Table 8: Total bone distribution expressed as percent of injected dose organ

| Organ | % ID/ organ<br>3-25-2010<br>Unconjugated<br>Tumor<br>Mean (SEM) | % ID/ organ<br>3-25-2010<br>Unconjugated<br>Control<br>Mean (SEM) | % ID/ organ<br>3-26-2010<br>PEG<br>Tumor<br>Mean (SEM) | %ID/organ<br>3-26-2010<br>PEG<br>Control<br>Mean (SEM) |
|---|---|---|---|---|
| Calvaria | 0.169(0.069) | 0.024(0.010) | 0.064(0.012) | 0.085(0.015) |
| Skull | 0.253(0.050) | 0.215(0.084) | 0.216(0.040) | 0.251(0.010) |
| Upper Spine | 0.197(0.052) | 0.183(0.080) | 0.403(0.104) | 0.327(0.048) |
| Lower Spine | 0.363((0.121) | 0.447(0.067) | 0.452(0.096) | 0.588(0.077) |
| Ribs | 0.186((0.053) | 0.133((0.053) | 0.222(0.050) | 0.206(0.013) |
| Right Arm | 0.089(0.011) | 0.064(0.023) | 0.079(0.015) | 0.108(0.021) |
| Left Arm | 0.325((0.275) | 0.060(0.023) | 0.092(0.026) | 0.092(0.014) |
| Right Leg | 0.365(0.317) | 0.182(0.079) | 0.139(0.025) | 0.222(0.043) |
| Left Leg | 0.367(0.335) | 0.156(0.070) | 0.168(0.053) | 0.184(0.034) |
| Tail | 8.489(6.147) | 10.612(8.525) | 12.752(5.537) | 9.642(5.911) |
| Total Bone | 10.804(5.987) | 12.075(8.114) | 14.587(5.533) | 11.706(5.742) |
| Total Bone<br>W/o Tail | 2.315(0.389) | 1.463(0.428) | 1.836(0.364) | 2.064(0.178) |

Table 9: Total bone distribution expressed as percent of injected dose organ

| Organ | % ID/ organ 3-29-2010 Targeted Tumor Mean (SEM) | % ID/ organ 3-29-2010 Targeted Control Mean (SEM) | % ID/ organ 4-5-2010 Targeted PEG Tumor Mean (SEM) | % ID/ organ 4-5-2010 Targeted PEG Control Mean (SEM) |
|---|---|---|---|---|
| Calvaria | 0.039(0.008) | 0.025(0.000) | 0.032(0.012) | 0.090 |
| Skull | 0.173(0.024) | 0.192(0.000) | 0.155(0.036) | 0.334 |
| Upper Spine | 0.228(0.030) | 0.289(0.005) | 0.172(0.033) | 0.259 |
| Lower Spine | 1.166(0.790) | 0.438(0.033) | 1.130(0.465) | 0.651 |
| Ribs | 0.133(0.014) | 0.157(0.025) | 0.101(0.021) | 0.187 |
| Right Arm | 0.051(0.008) | 0.070(0.007) | 0.044(0.013) | 0.092 |
| Left Arm | 0.047(0.009) | 0.062(0.008) | 0.041(0.009) | 0.079 |
| Right Leg | 0.105(0.018) | 0.131(0.004) | 0.091(0.029) | 0.212 |
| Left Leg | 0.090(0.013) | 0.117(0.007) | 0.079(0.022) | 0.155 |
| Tail | 12.765(5.068) | 5.571(1.133) | 15.005(4.183) | 7.598 |
| Total Bone | 14.798(5.385) | 7.051(1.084) | 16.849(4.295) | 9.655 |
| Total Bone W/o Tail | 2.033(0.790) | 1.480(0.049) | 1.845(0.425) | 2.058 |

At the end of the study, we also collected the limbs and spines from both GFP tumor and control mice into paraformaldehyde and scanned them in an optical imaging system. Images for four different mice injected with GFP tumor cells are attached (Figure 20-23). There is fluorescence covering the spine as well as discrete uptake in the limbs of mouse 4.

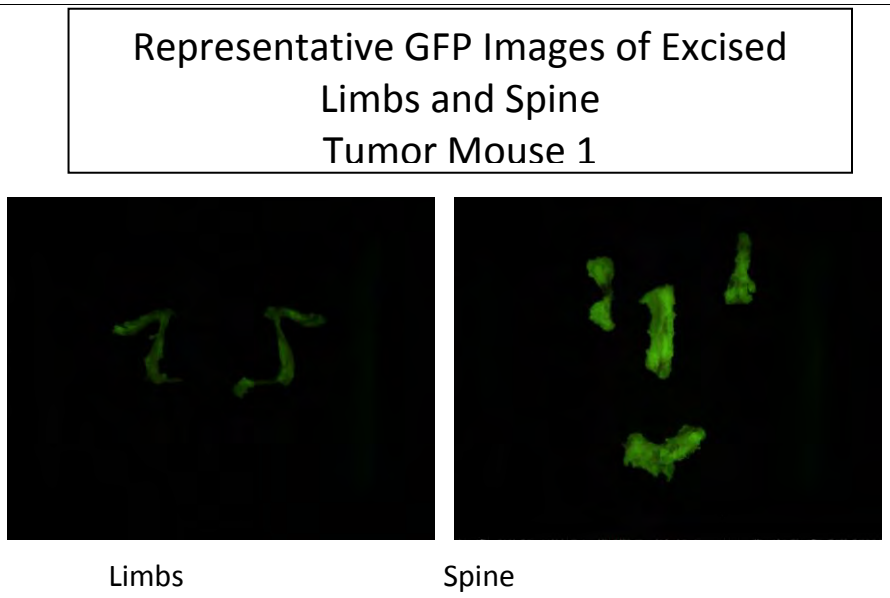


**Figure 20:** Limbs and spine of GFP labeled tumor cells in mouse

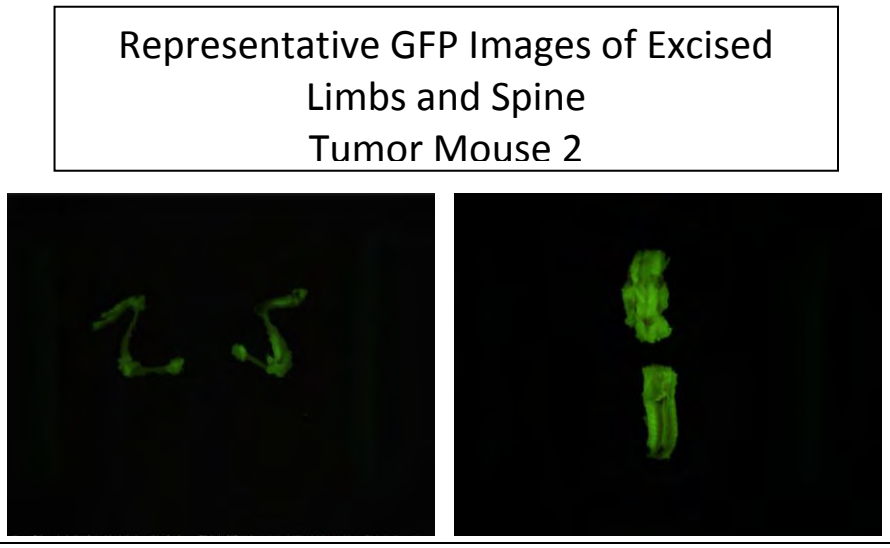


**Figure 21:** Limbs and spine of GFP labeled tumor cells in mouse

| | |
|---|---|
| Representative GFP Images of Excised Limbs and Spine<br>Tumor Mouse 3<br> 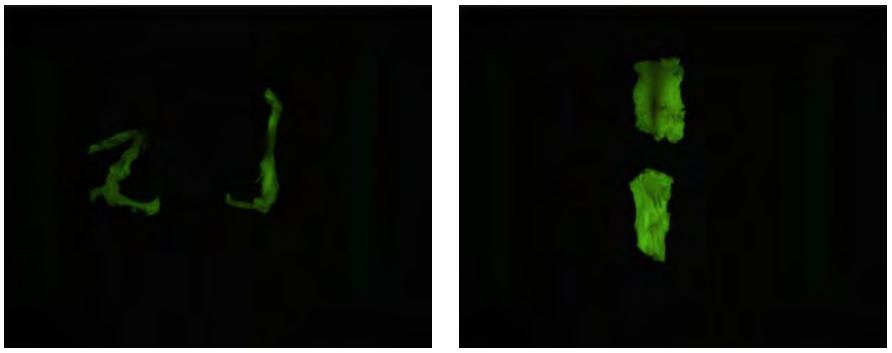 <br>Limbs Spine | **Figure22:** Limbs and spine of GFP labeled tumor cells in mouse |
| Representative GFP Images of Excised Limbs and Spine<br>Tumor Mouse 4<br> 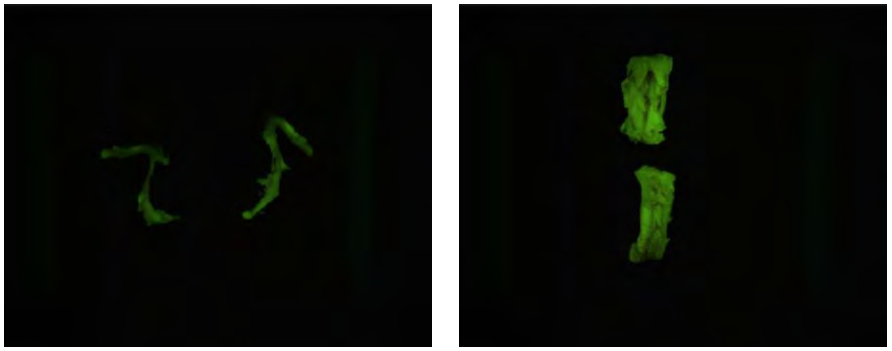 <br>Limbs Spine | **Figure 23:** Limbs and spine of GFP labeled tumor cells in mouse |

Representative planar images of each group acquired at various time points after intravenous injection are attached (Fig 24-31). For each time point and formulation, the organ with the most $^{99m}$Tc-activity is the liver.

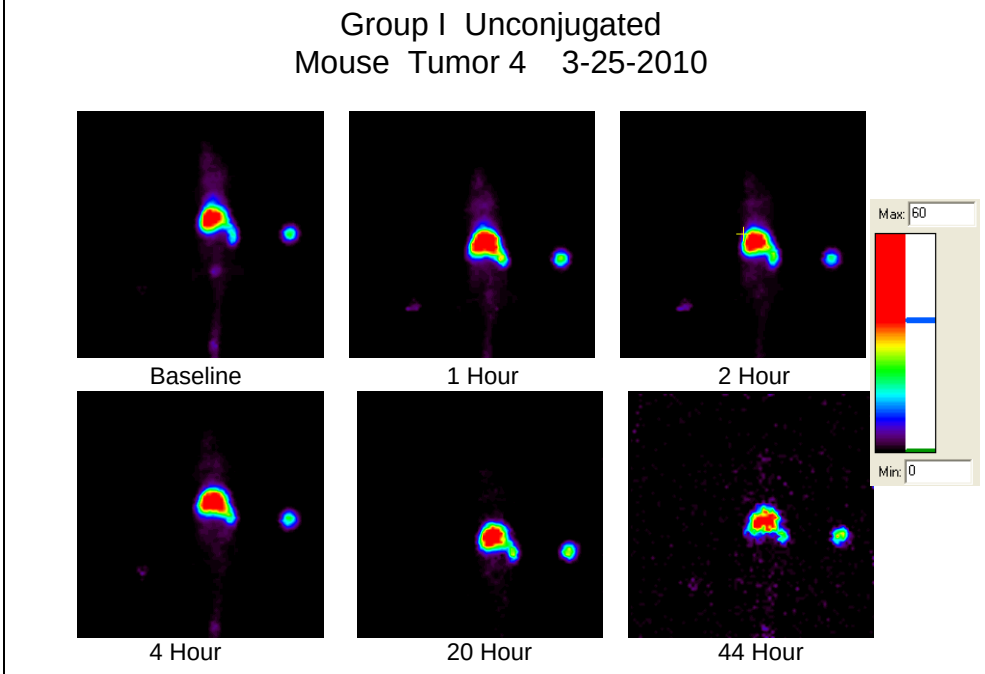


**Figure 24:** Planar image of mice injected with 5% PEG Non-Targeted at various time points

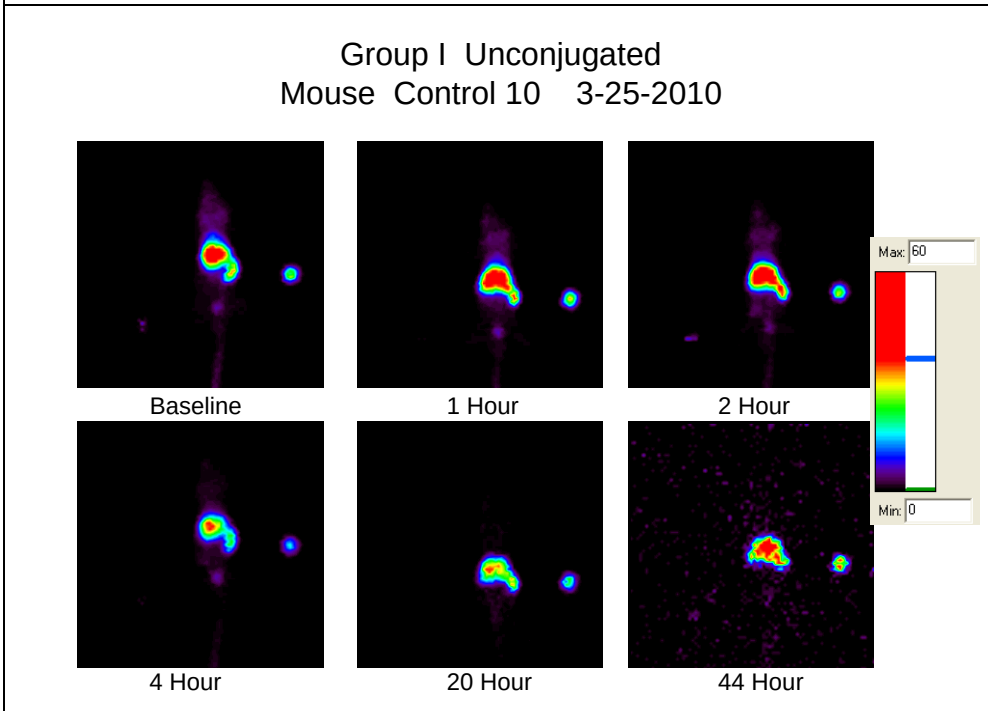


**Figure 25:** Planar image of mice injected with 5% PEG Non-Targeted at various time points

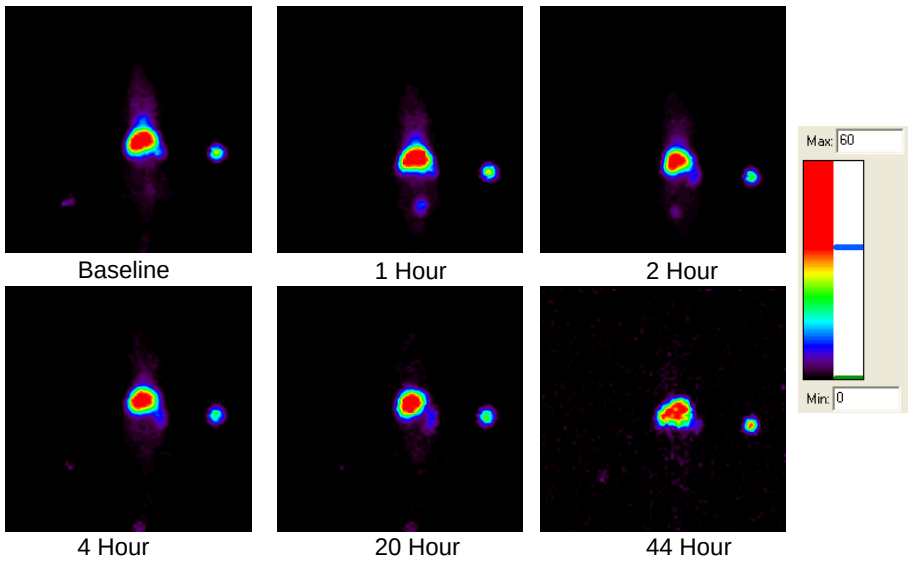


**Figure 26:** Planar image of mice injected with 15% PEG Non-Targeted at various time points

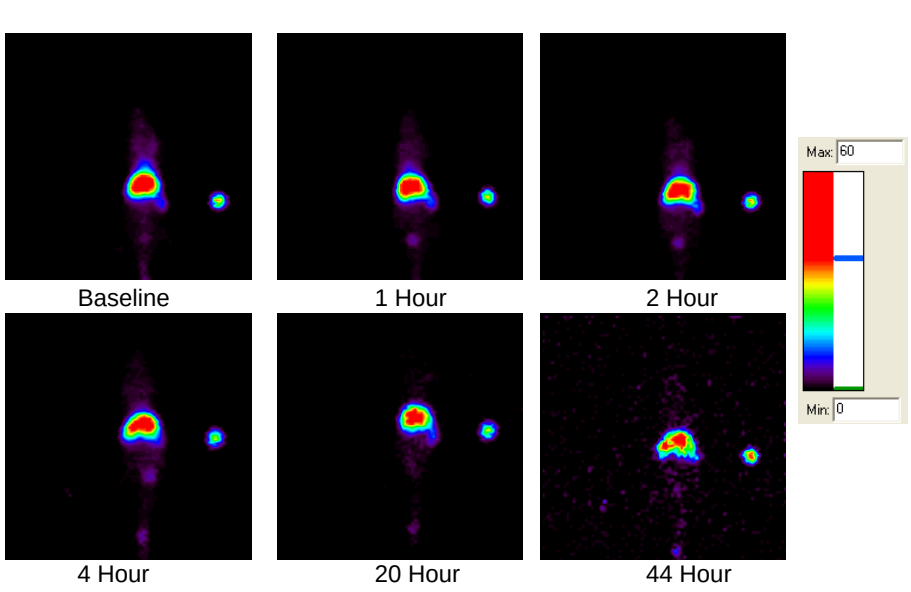


**Figure 27:** Planar image of mice injected with 15% PEG Non-Targeted at various time points

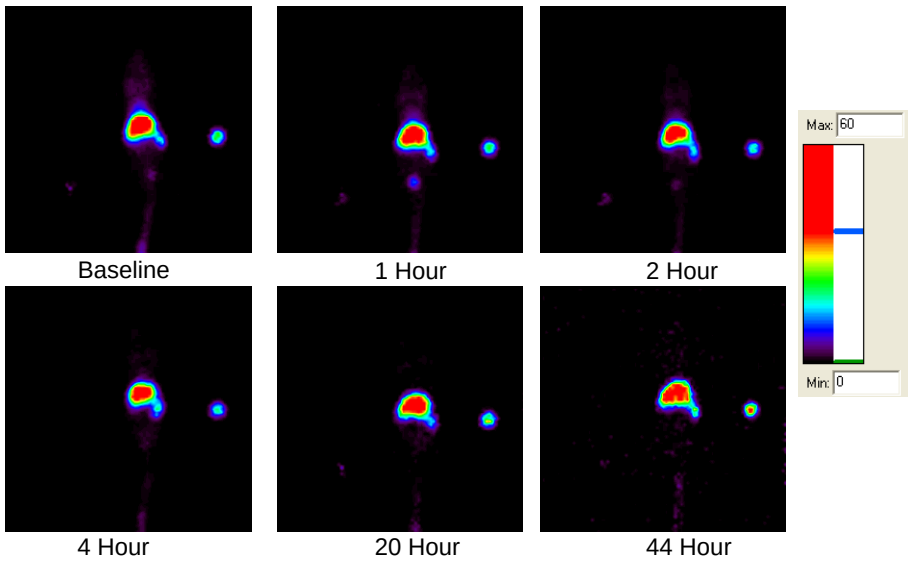


**Figure 28:** Planar image of mice injected with 5% PEG Targeted at various time points

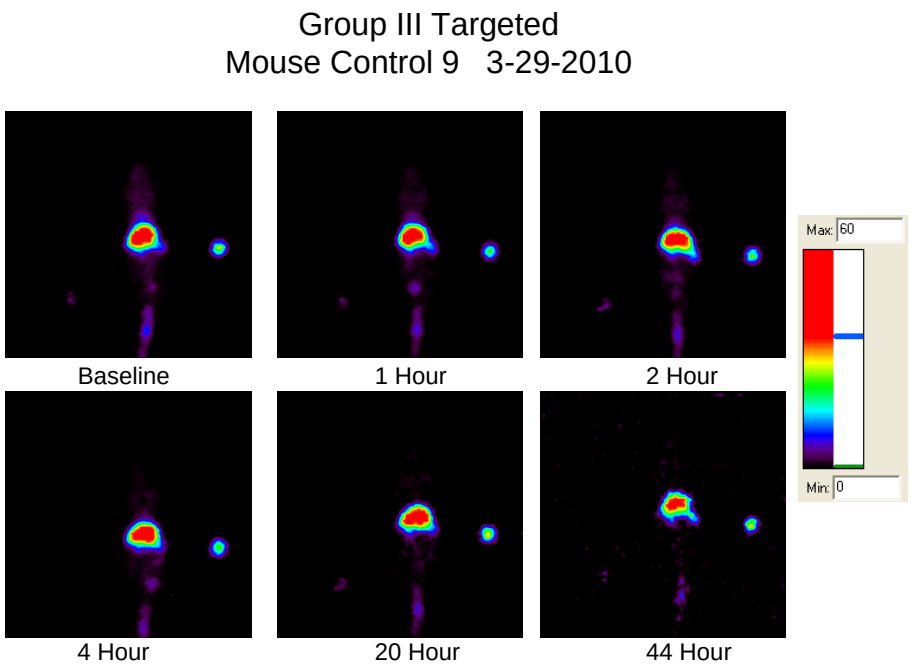


**Figure 29:** Planar image of mice injected with 5% PEG Targeted at various time points

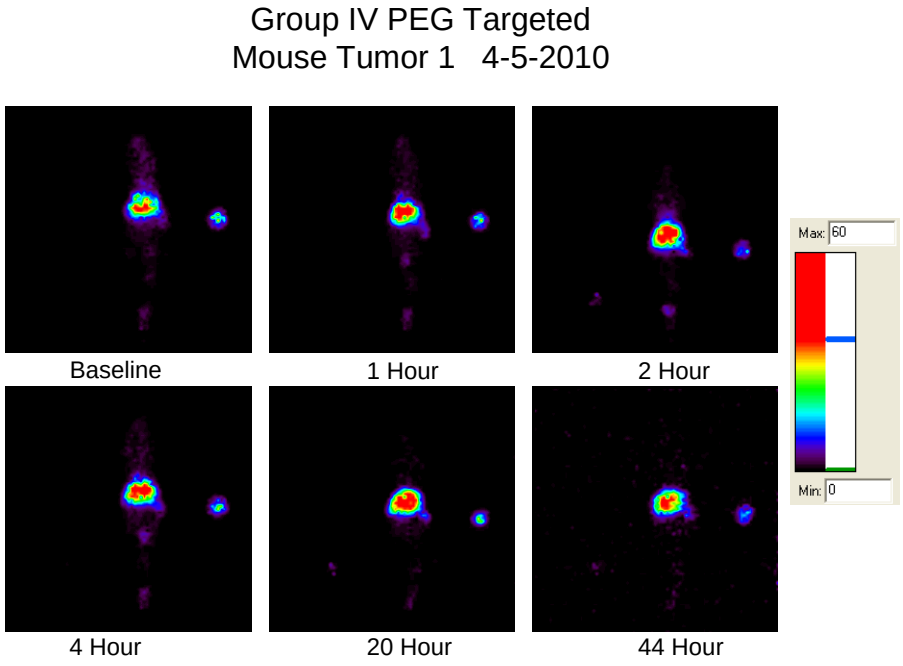


**Figure 30:** Planar image of mice injected with 15% PEG Targeted at various time points

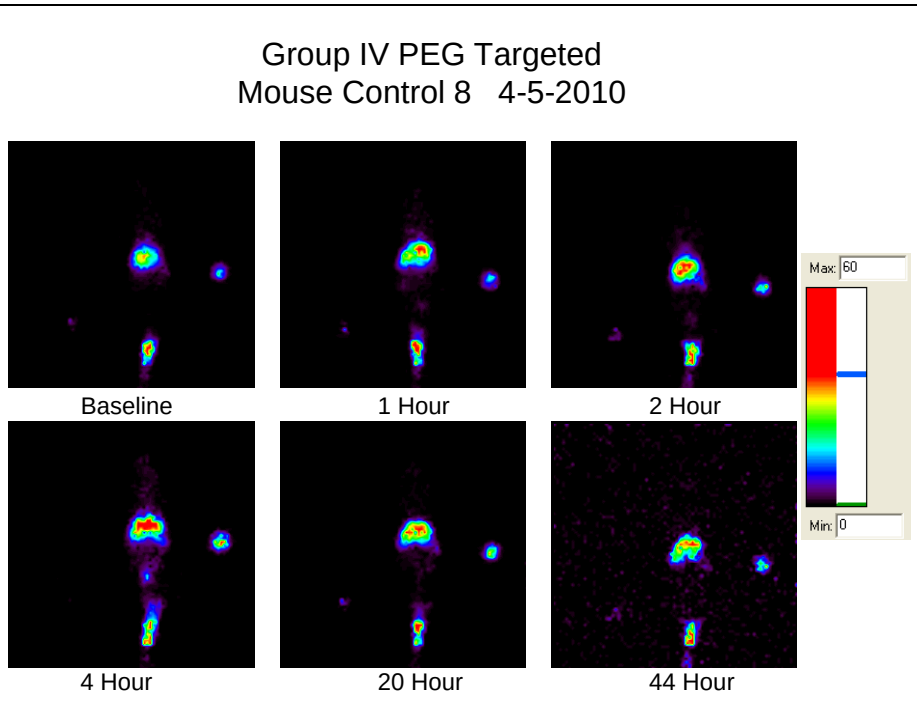


**Figure 31:** Planar image of mice injected with 15% PEG Targeted at various time points

Figures 32-35 show whole body biodistribution of two nanoparticles formulations, one for 5% PEG and one for 15% PEG composition, of bone targeted and non targeted nanoparticles. Figures 36-39 demonstrated bone biodistribution of the above mentioned nanoparticles (5 and 15% PEG composition targeted and non targeted) Figures 40-43 demonstrate blood clearance of the above mentioned formulations

Biodistribution of non-targeted and targeted NPs is shown in figures below:

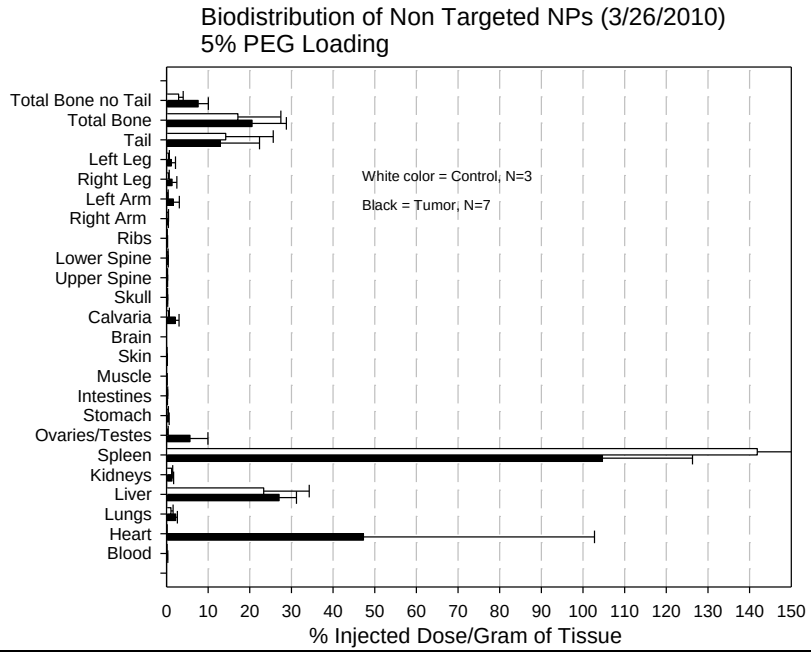


**Figure 32:**
Whole body biodistribution of 5% PEG loaded Non-Targeted PLGA-PEG NPs. White bars are control mice and black bars are tumor-bearing mice.

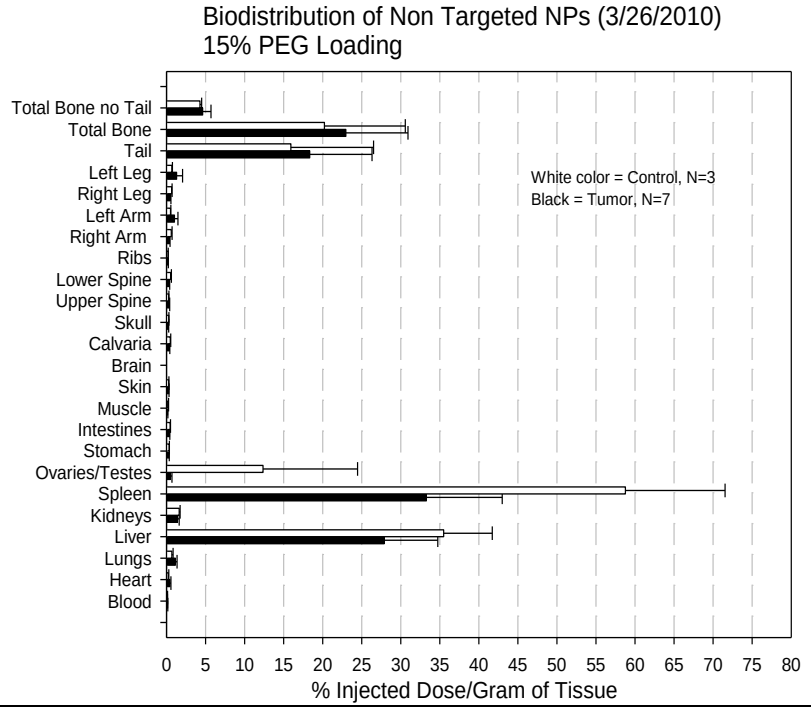


**Figure 33:**
Whole body biodistribution of 15% PEG loaded Non-Targeted PLGA-PEG NPs. White bars are control mice and black bars are tumor-bearing mice.

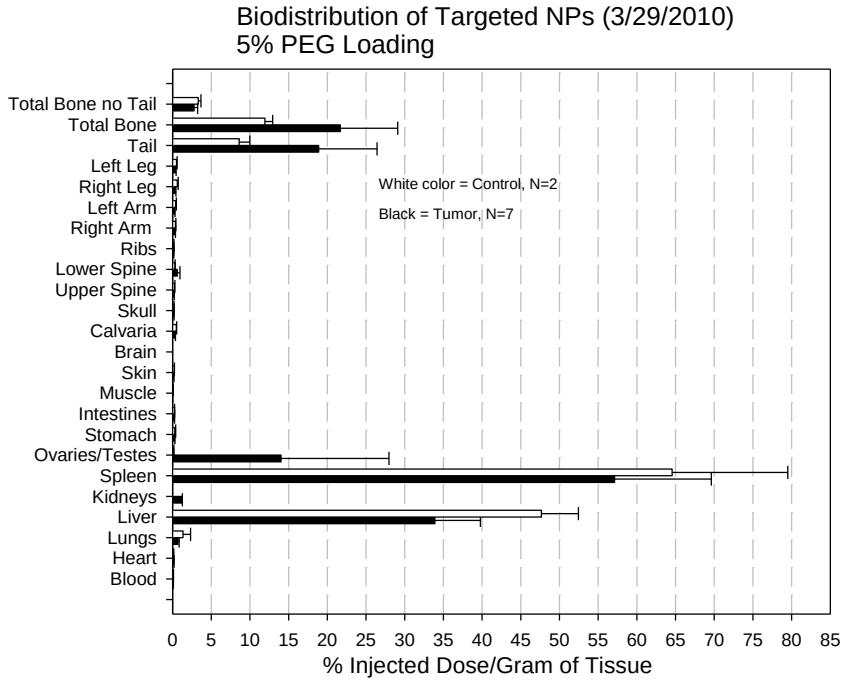


**Figure 34:**
Whole body biodistribution of 5% PEG loaded Targeted PLGA-PEG NPs. White bars are control mice and black bars are tumor-bearing mice.

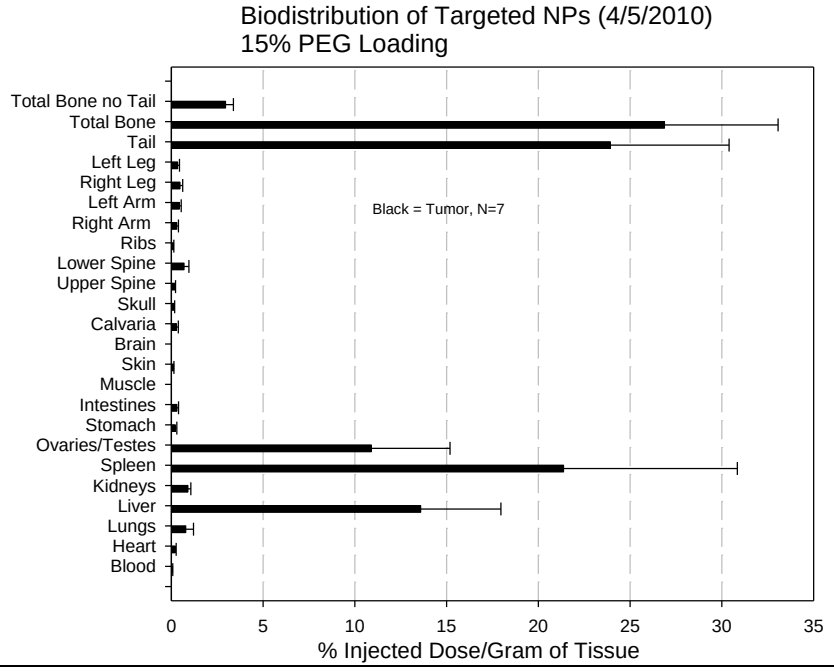


**Figure 35:**
Whole body biodistribution of 15% PEG loaded Targeted PLGA-PEG NPs. black bars are tumor-bearing mice.

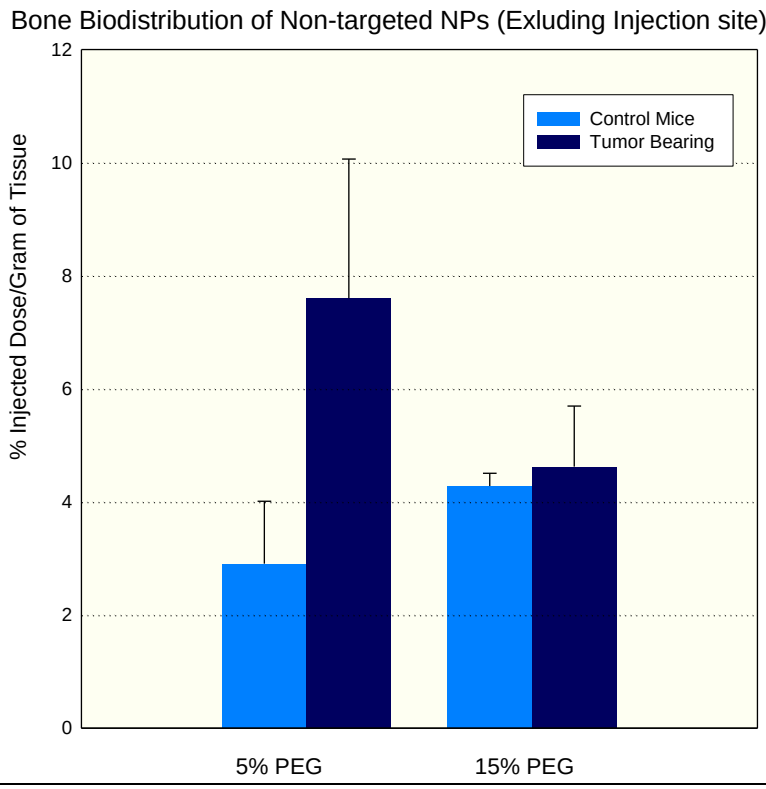


**Figure 36:**
Bone biodistribution of 5% and 15%PEG Non-Targeted PLGA-PEG NPs. Light blue bars are control mice and dark blue are tumor-bearing mice

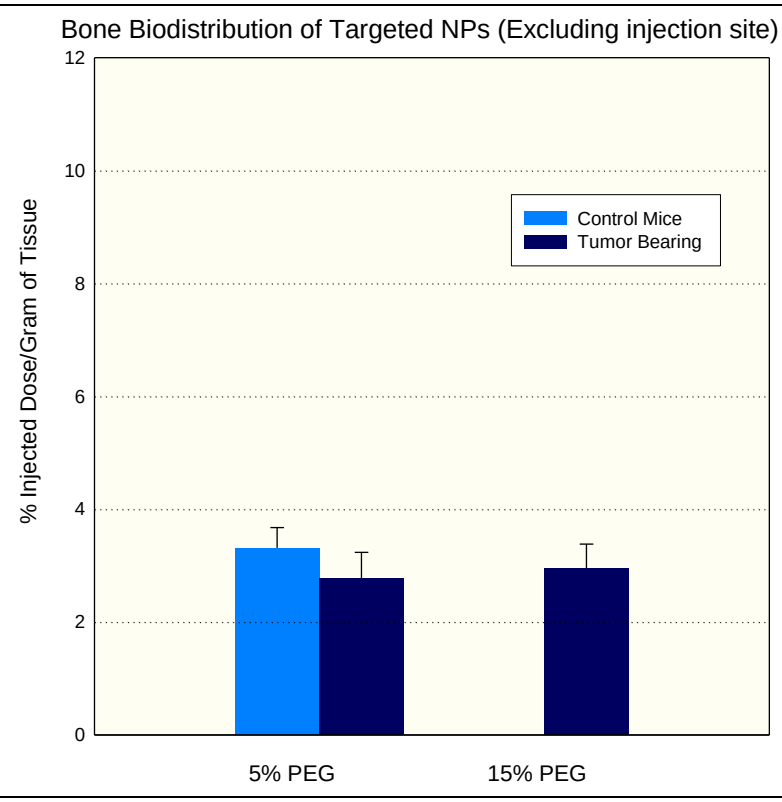


**Figure 37:**
Bone biodistribution of 5% and 15% PEG Non-Targeted PLGA-PEG NPs. Light blue bars are control mice and dark blue are tumor-bearing mice. (missing bar due to data no available)

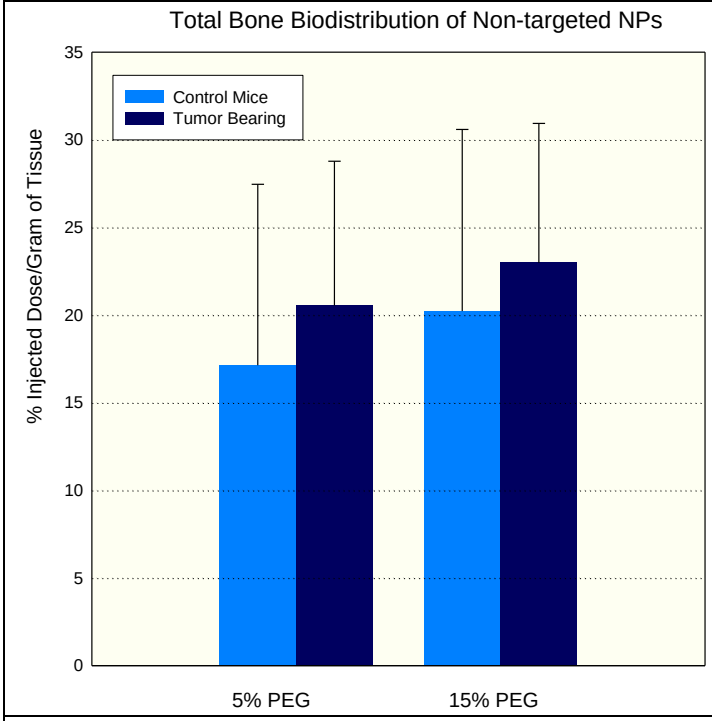


**Figure 38:**
Bone biodistribution of 5% PEG Targeted PLGA-PEG NPs. Light blue bars are control mice and dark blue are tumor-bearing mice.

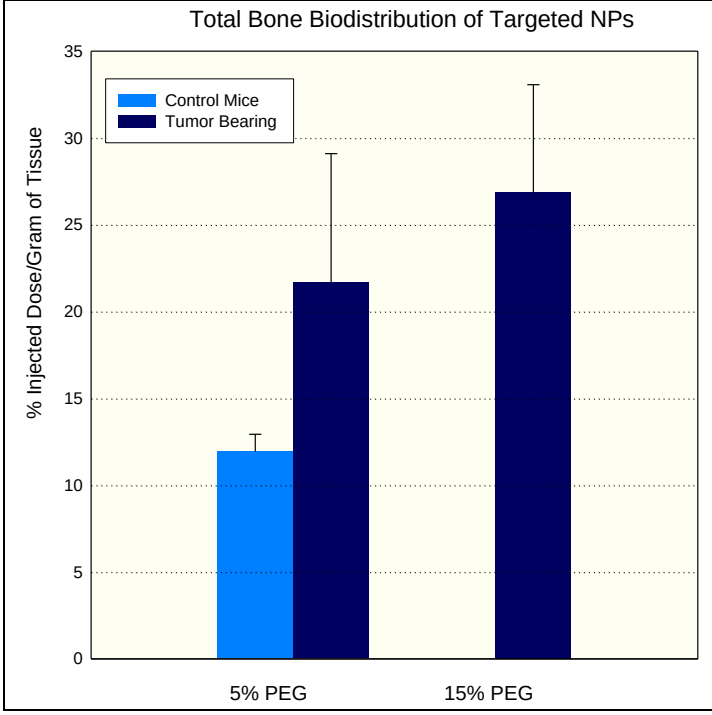


**Figure 39:**
Bone biodistribution of 15% PEG Targeted PLGA-PEG NPs. Light blue bars are control mice and dark blue are tumor-bearing mice.

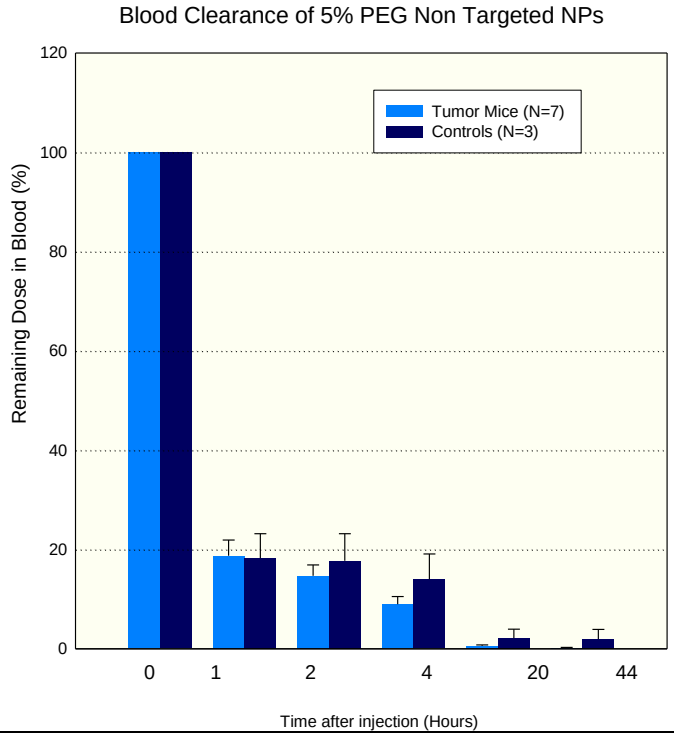


**Figure 40:**
Blood clearance of 5%PEG Non Targeted Nanoparticles in control and tumor-bearing mice.

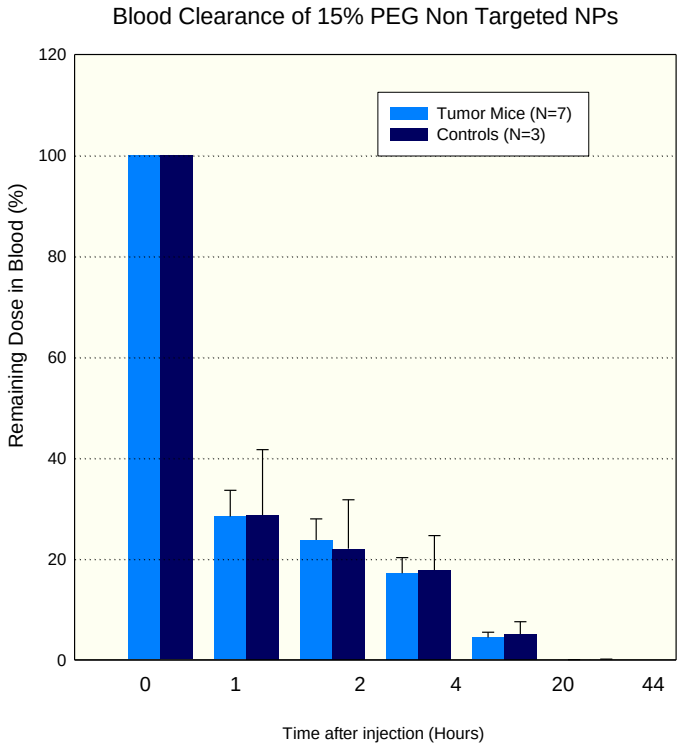


**Figure 41:**
Blood clearance of 15%PEG Non Targeted Nanoparticles in control and tumor-bearing mice.

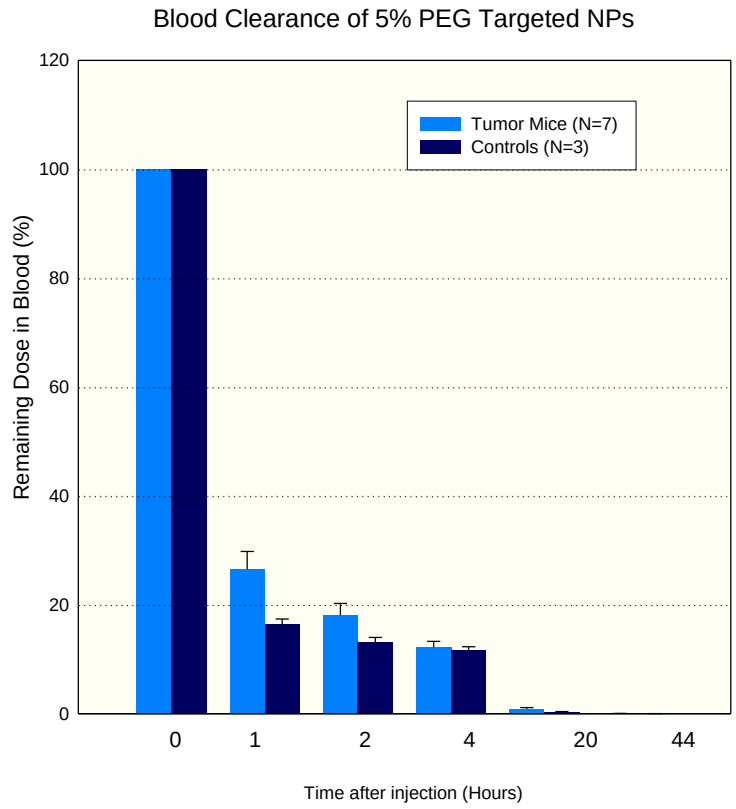


**Figure 42:**
Blood clearance of 5%PEG Targeted Nanoparticles in control and tumor-bearing mice.

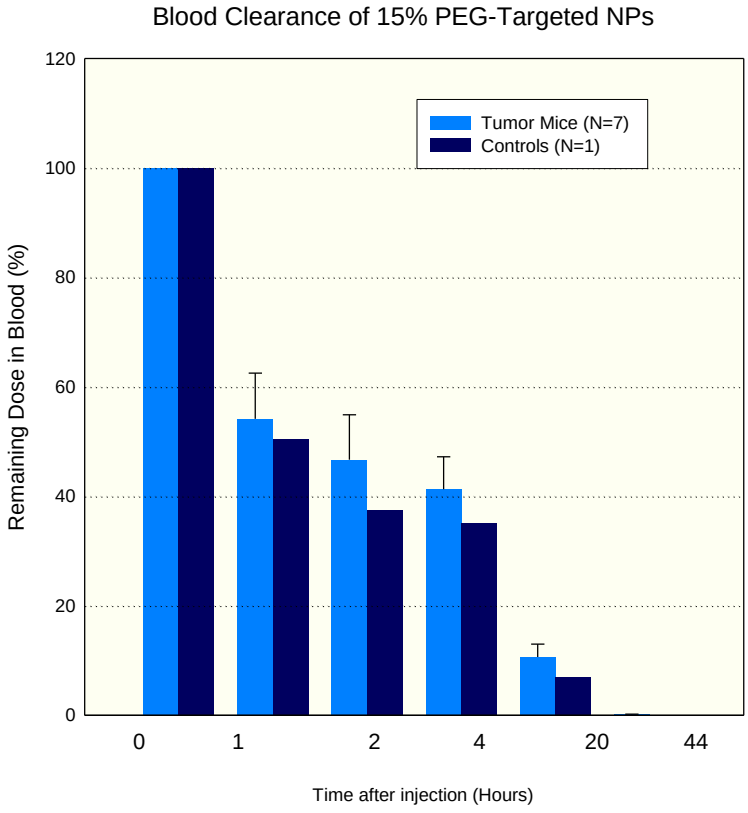


**Figure 43:**
Blood clearance of 15%PEG Non Targeted Nanoparticles in control and tumor-bearing mice.

3) Task 3 is concerned with demonstrating the efficacy of bone-targeting nanoparticles containing small molecule therapies in a myeloma mouse model. The task is broken down into the following subtasks:

- Prepare drug loaded bone-targeting nanoparticles. Pending.
- Conduct *in vivo* efficacy studies. Pending.

## 3. KEY RESEARCH ACCOMPLISHMENTS

Year 1:

1. Synthesized amino-functionalized methylene bisphosphonate to serve as one of two bone-targeting ligands to be attached to polymer nanoparticles.

2. Developed two procedures for preparing nanoparticles and demonstrated their ability to repeatedly produce nanoparticles with narrow distribution in the target particle size range of 100-200nm and smaller, if necessary.

3. Synthesized PLGA-b-PEG block copolymers to prepare PEGylated nanoparticles with improved circulatory half-lives.

4. Formulated PEGylated nanoparticles using available procedures.

5. Synthesized PLA-b-PEG-Maleimide block copolymers to facilitate the attachment of bone-targeting ligands to polymer nanoparticles via thiol coupling.

6. Developed methods of stabilizing polymer nanoparticles, with and without PEG modification, against cryoprocessing.

7. Confirmed adsorption of selected bone-targeting ligands to bone-like substrates in vitro and established ligand coupling chemistry.

8. Selected proteasome inhibitors for upcoming studies.

9. Encapsulated model proteasome inhibitor, MG-132.

10. Established proteasome inhibitor assay for determining nanoparticle payloads.

11. Developed animal protocols for upcoming in vivo studies in Tasks 2 and 3.

Year 2:

1. Developed two procedures for preparing nanoparticles and demonstrated their ability to repeatedly produce nanoparticles with narrow distribution in the target particle size range of 70-200nm and smaller, if necessary.

2. Synthesized and fully characterized PLA-b-PEG-Maleimide block copolymers to facilitate the attachment of bone-targeting ligands to polymer nanoparticles via thiol coupling.

3. Improved lyostability of polymer nanoparticles, with and without PEG modification.

4. Developed methods to radiolabel polymer nanoparticles, the first time, to our knowledge, this has been done.

5. Encapsulated two proteasome inhibitors, MG-132 and PS-1, and determined their in vitro release profiles.

6. Developed proteasome activity assay to determine activity of encapsulated drug.

7. Developing in vitro assay to determine affinity of bone-targeting nanoparticles to hydroxyapatite substrates.

Year 3:

1. Developed methods to radiolabel polymer nanoparticles, the first time, to our knowledge, this has been done.

2. Quantified functional groups available for ligand conjugation using S35-labeled ligands.

3. Developed alternative assay to confirm affinity of bone-targeting nanoparticles to hydroxyapatite substrates.

4. Demonstrated in vitro stability of radio-labeled nanoparticles.

5. Successfully transferred our nanoparticle preparation protocols to another facility to support in vivo biodistribution studies.

6. Started in vivo biodistributions, validating ability of our radio-labeled nanoparticles to be imaged for up to 48 hours and further confirming our protocol methods to study bone-targeting nanoparticle biodistribution via radio-imaging.

Year 4:

1. Developed methods to radiolabel polymer nanoparticles; to our knowledge, this is the first time this has been accomplished.

2. Quantified functional groups available for ligand conjugation using OPA amino reagent.

3. Developed alternative assay to confirm affinity of bone-targeting nanoparticles to hydroxyapatite substrates.

4. Demonstrated *in vitro* stability of radio-labeled nanoparticles.

5. Successfully transferred our nanoparticle preparation protocols to another facility to support *in vivo* biodistribution studies.

6. Started *in vivo* biodistribution studies to validate ability of our radio-labeled nanoparticles to be imaged for up to 48 hours and further confirming our protocol methods to study bone-targeting nanoparticle biodistribution via radio-imaging.

## 4. REPORTABLE OUTCOMES

Year 1:

1. Abstract submitted to DoD-USAMRMC/PRMRP Military Health Research Forum.

2. Invited to present results from this program at talk at the Particles 2006 –Medical/Biochemical Diagnostic, Pharmaceutical, and Drug Delivery.

3. Applications of Particle Technology Forum scheduled for May 13 –16, in Orlando, FL.

4. Invited to give a guest lecture on nanoparticle drug delivery technology to the Graduate Bioengineering Program at the University of Texas at San Antonio, March, 2006.

5. Provided an opportunity for a high school student through the Project SEED.

6. Program of the American Chemical Society. The program is geared to expose under-represented and disadvantaged high school students to chemistry to encourage their continued education.

7. Hired a PhD Bioengineering student who's thesis will be based on work conducted on this project.

8. Subcontract in place with UTHSC for the biodistribution study described in Task 2 scheduled for the coming year.

Year 2:

1. Abstract accepted to Society of Biomaterials Annual Meeting.

2. Two abstracts submitted to the Annual Meeting of the Controlled Release Society.

3. Invited to present work to the 59th Annual Meeting of the Board of Directors of Southwest Research Institute.

4. Hired additional professional staff who have been instrumental in completing nanoparticle formulation work and will be supporting upcoming biodistribution studies.

5. Subcontract executed for biodistribution study with UTHSC-SA described in Task 2.

6. Animal protocols for the biodistribution and efficacy studies described in the original statement of work (Tasks 2 & 3, respectively) have been reviewed and approved by the DoD Animal Care & Use Review Office.

Year 3:

1. Manuscript in preparation discussing the development of bone-targeting nanoparticles and radio-labeled nanoparticles.

2. Presented poster at 32nd Annual Meeting of the Society of Biomaterials.

3. Made podium presentation entitled "Development and Characterization of Bone- Targeting Nanoparticles" at the 34th Annual Meeting of the Controlled Release Society, July 7 – 11, Long Beach, CA.

4. Presented poster entitled "Controlled Release of Proteasome Inhibitor from Biodegradable Nanoparticles for Myeloma Therapies" at the 34th Annual Meeting of the Controlled Release Society, July 7 – 11, Long Beach, CA.

5. Hired additional professional staff to support biodistribution and in vivo efficacy studies.

6. Animal protocols for the biodistribution and efficacy studies described in the original statement of work (Tasks 2 & 3, respectively) have been reviewed and approved by the DoD Animal Care & Use Review Office.

Year 4:

1. A change of the principal investigator (PI) was filled this year due to the departure of the previous PI.

2. An extension for final completion of this project was granted by the U.S. Army Office. The new completion date is now on March 17, 2010.

3. Animal protocols for the biodistribution and efficacy studies described in the original statement of work (Task 2) have been reviewed and approved by the IACUC office and the ACURO army office.

4. An abstract was submitted and accepted for presentation at the annual CDMRP conference in Kansas City, Missouri in September 2009. Abstract provided in appendix 3.

## 5. CONCLUSIONS

We completed extensive nanoparticle formulation work at the bench level and performed several biodistribution studies of the best formulations. We consistently prepared polymer nanoparticles of required size and composition necessary to support other tasks of the project.

We formulated Velcade for prolonged release using long circulating PLGA-PEG nanoparticles, and demonstrated partial bone accumulation of the targeted nanoparticles *in vitro* and *in vivo.* At the time of this final report preparation we initiated the final efficacy studies. So far, we have done three out of four weeks dosing of targeted and non targeted nanoparticles formulated with Velcade at 0.6 and 3.0 mg/kg total dose. Controls include the same doses as free saline formulated drugs, empty nanoparticles, and saline vehicles.

The *in vivo* results demonstrate that after 4 hours, we can expect 50% of the nanoparticles to still be in circulation.

Bone targeting was only partially achieved (a 3-fold increase over non targeted nanoparticles); however, this small increase may result in a dramatic efficacy improvement. Also, the additional benefits include simplifying the dosing and avoiding toxic solvents used with some of the chemotherapeutics.

In vivo efficacy studies are presented in Appendix 4. This study was done in collaboration with UTHSCSA (Professor Babatunde O. Oyajobi at UTHSCSA) and interpretations of results are presented by him.

## 6. REFERENCES

Mundy, G. R. Myeloma bone disease. In: Bone Remodeling and Its Disorders. London: Dunitz; 1995; 123:136.

I.Garrett, S.Dallas, J.Radl, G.Mundy: A murine model of human myeloma bone disease *2007 Bone* 20 (6): 515-520.

Ahmedin Jemal, PhD, DVM, Taylor Murray, Alicia Samuels, MPH, Asma Ghafoor, MPH, Elizabeth Ward, PhD and Michael J. Thun, MD, MS **2003 Cancer Statistics, Cancer J Clin 2003; 53:5.**

Kasugai S, Fujisawa R, Waki Y, Miyamoto K, Ohya K 2000 Selective drug delivery system to bone: small peptide (Asp)6 conjugation. J Bone Miner Res 15:936–943.

"Zeta Potential of Colloids in Water and Waste Water", ASTM Standard D 4187-82, American Society for Testing and Materials, 1985.

# Appendices

## **APPENDEX 1:** Synthesis of PLA-b-PEG-Ligand

The bone-targeting capability of our nanoparticles was provided by covalently attaching previously identified ligands to the nanoparticles surfaces via an activated polyethylene glycol (PEG) linker. Our approach to preparing this linker was to start with a bifunctional PEG and selectively attach to the respective ends either the bone-targeting ligand or a polylactide polymer.

As reported previously, we were able to procure the required bifunction PEG from a commercial source. This material has the form HO-PEG-$NH_2$ with the PEG segment being approximately 3400 molecular weight. The synthetic approach was to couple the PLA segment to the PEG block via the HO- moiety, leaving the –$NH_2$ moiety for attaching the Ligand.

The first step was to attach PLA to the bifunctional PEG using ring-opening polymerization in the presence of a coordination catalyst as illustrated in Figure 3 (see Scheme 1). The amine group (-$NH_2$) is protected during the polymerization. Using tin 2-ethylhexanoate as a catalyst and lactide monomer, we prepared PLA-b-PEG-NH2 block copolymer and confirmed the structure and composition of the recovered product by $^1$H-NMR. In one example, the resulting molecular weight of the PLA block was estimated to be about 25,500. The PLA block length can be altered by adjusting the catalyst content using an inverse relationship based on the polymerization kinetics. We obtained PLA blocks of approximately 44,000 molecular weight by simply reducing the amount of catalyst. This particular block length is essentially equivalent to the molecular weight of the PLGA polymers used in the base nanoparticle formulation.

Bone-targeting ligands were covalently attached to the PEG linker via a thiol coupling to a maleimide group (see Scheme 3, Figure 3). The maleimide group was introduced to the –NH2 terminus of the previously prepared PLA-b-PEG material by reaction with 3-maleimidopropionic acid N-hydroxysuccinimide ester (MPS). We discovered that the maleimide functionalization could not be achieved using the PLA-b-PEG-$NH_2$ starting material. Alternatively, we found it necessary to first attach the maleimide group to the HO-PEG-$NH_2$, followed by PLA attachment to the HO-PEG-Maleimide by the previously described ring-opening polymerization. Structures were confirmed at each of the key synthesis points by $^1$H-NMR. The typical product had a PLA block size of about 52,000 molecular weight.

Our next step in this development was to attach the selected bone-targeting ligands to these maleimide-functionalized block copolymers. Both of the selected ligands, amino methylene bisphosphonate (aMBP) and an aspartic acid oligomer ($Asp_n$), have an amino terminus. This is converted to thiol by reaction with Traut's Regeant (2-iminothiolane, see Scheme 2, Figure 3). This thiol analogue then reacts with the maleimide moiety of the block copolymer to yield a covalently attached ligand.

**Scheme 1 - Synthesis of Polyethylene glycol - polylactide-co-galactide Block Copolymers**

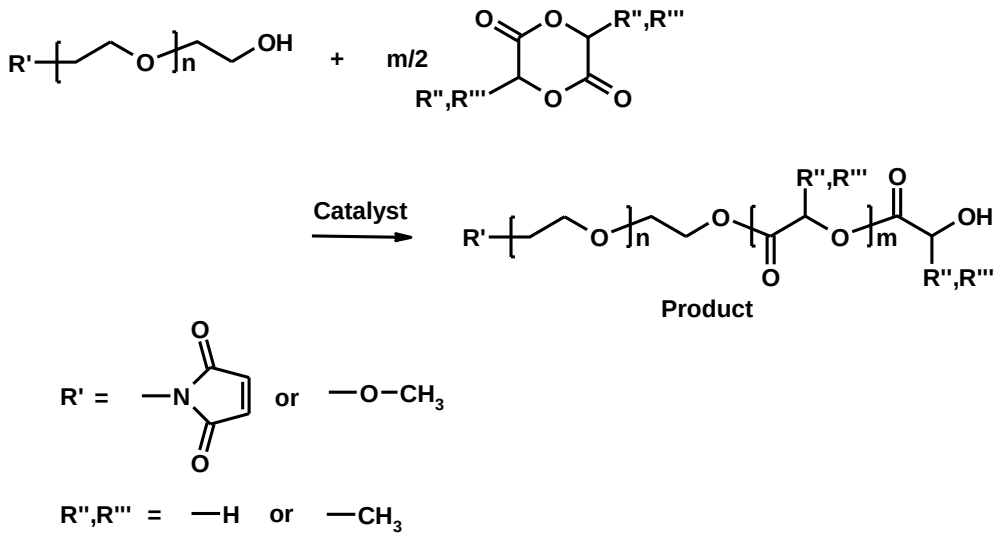


**Scheme 2 - Thiolation of Amino-terminated Bone-targeting Ligands**

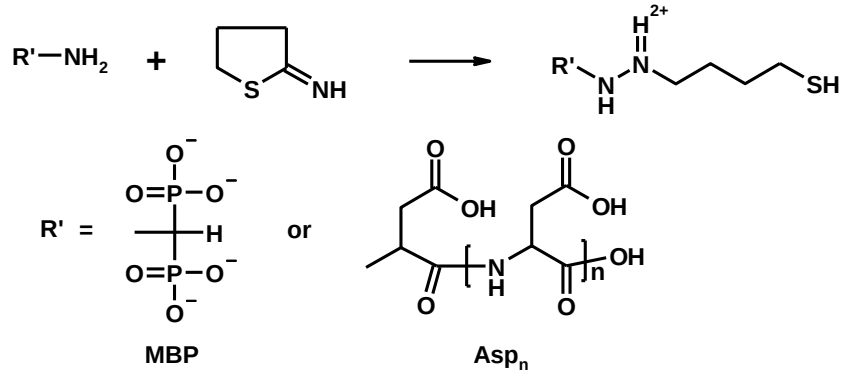


**Scheme 3 - Conjugation of Thiolated Bone-targeting Ligands to PEG-Lactide Block Copolymers**

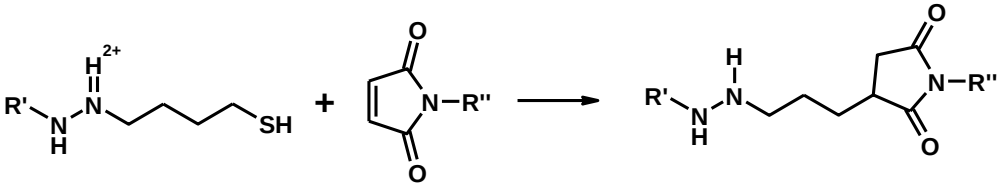


**R' = See Scheme 2 above**
**R" = Product from Scheme 1 above**

**Figure 3.** Synethic schemes for the preparation of PEGylated polylactide block copolymers (Scheme 1), thiolation of amino-terminated bone-targeting ligands (Scheme 2), and, conjugation of thiolated bone-targeting ligands to maleimide-functionalized PEGylated polylactide block copolymers (Scheme 3).

Synthesis of PLA-b-PEG-Ligand

The materials mentioned above were analyzed by $^1$H-NMR to determine their composition and product yield. The starting material for this synthesis was the bifunctional PEG, HO-PEG-$NH_2$, with the PEG segment having an estimated molecular weight of 3400. Figure 4 shows the $^1$H-NMR spectrum of this material. The methylene groups of the PEG block have a shift of $\delta$ ~ 3.6ppm and the methylene group adjacent the terminal amine, -$NH_2$, has a shift of $\delta$ ~ 2.8ppm. The hydrogen balance of these peaks is a follows:

$$\frac{4n+2}{2} = \frac{a}{b}$$

where *n* is the PEG block length, *a* the integrated peak height of the PEG methylene groups, and *b* the integrated peak height of the methylene group adjacent the terminal amine. This leads to a block length of approximately 85, corresponding to a PEG molecular weight of about 3750, in good agreement with the suppliers' estimate.

We noted in previous work that it was best to first attach the maleimide functional group necessary for thiol-mediated coupling of our ligands followed by the attachment via ring-opening polymerization of a polylactic acid block. The first step is achieved according to the scheme shown in Figure 5 followed by isolation of the product in diethylether. Figure 6 shows the $^1$H-NMR spectrum of the isolated product. Similar compositional analysis to that of the PEG starting material can be applied to determine the extent of maleimide attachment. The relevant peaks are the PEG methylene hydrogens at $\delta$ ~ 3.6ppm and the maleimide hydrogens at $\delta$ ~ 6.7ppm. The hydrogen balance is a follows:

$$\frac{4n+2}{2} = \frac{a}{b}$$

This leads to a PEG block length, n, of about 201 units. The ratio of the known block length determined previously to this value is an estimate of the extent of maleimide coupling, which is 85/201 = 42%. This conversion is low and we then considered other reaction conditions to increase the conversion.

After maleimide attachment, a polylactic acid block was attached via ring-opening polymerization followed by precipitation into water. This chemistry has been discussed in previous reports. Figure 7 shows the $^1$H-NMR spectrum of the isolated product. The PLA block length is estimates as follows:

$$\frac{4n+2}{3m+3} = \frac{a}{c}$$

where *n* and *m* are the PEG and PLA block lengths, respectively, *a* the integrated peak height of the PEG methylene hydrogens, and *c* the integrated peak height of the lactic acid methyl group. The PEG block length, *n*, is known from previous analysis leading to an estimate of the PLA block length of 830. This corresponds to PLA block molecular weight of about 60,000, which is similar in length to our neat PLA and PLGA commercial polymers. Further analysis of the product spectrum indicated the continued presence of the maleimide functional group, although the amount of this component relative to the original starting material has not been fully quantified.

The maleimide-functionalized PEG-b-PLA block copolymer was formulated into nanoparticles to develop a method to quantify the amount of functional groups available for bone-targeting ligand attachment. This was necessary to be able to prepare nanoparticles with different amounts of ligands to ascertain the effect of ligand content on the ability of the particles to target.

The functional polymer was mixed with PLGA in a ratio of 10/90 w/w, corresponding to an estimated functional group content of about 5nmol. Particles were precipitated and solvent removed by crossflow

filtration according to procedures described previously. These particles were incubated with a thiol-containing fluorescent probe (SAMSA, (5-((2-(and-3)-S-(acetylmercapto) succinoyl) amino) fluorescein) fluorescein, Molecular Probes) for 30 minutes after which the particles were separated by centrifugal dilation. Material balance on the fluorescent probe indicated a functional group content of about 3.05nmol, in reasonable agreement with the estimated content.

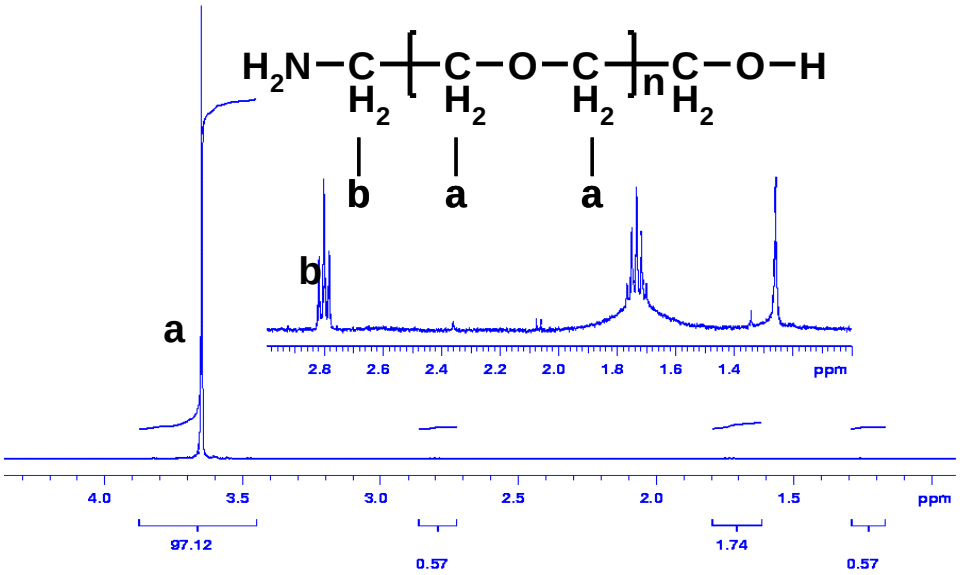


**Figure 4.** 1H-NMR spectrum of commercially available bifunctional polyethylene glycol.

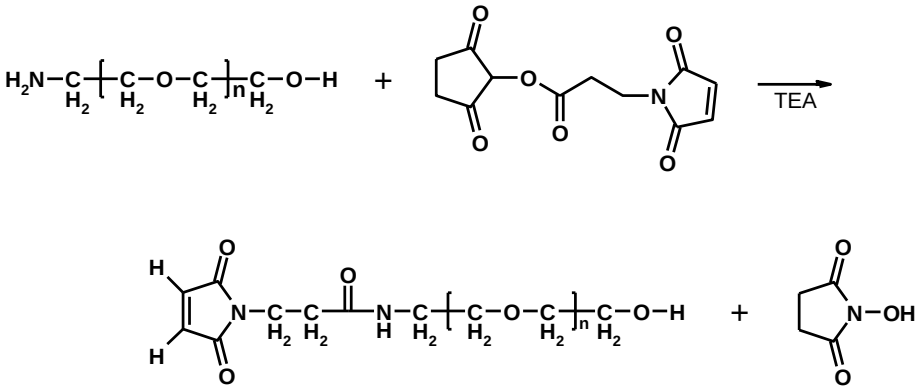


**Figure 5:** Reaction scheme for the maleimide functionalization of a bifunctional polyethylene glycol.

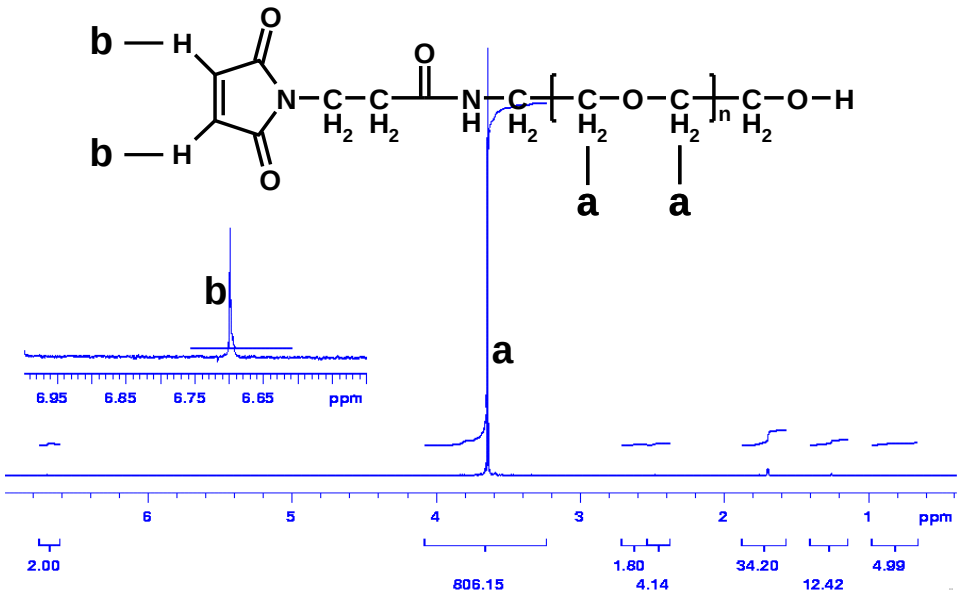


**Figure 6:** 1H-NMR spectrum of maleimide-coupled bifunctional PEG.

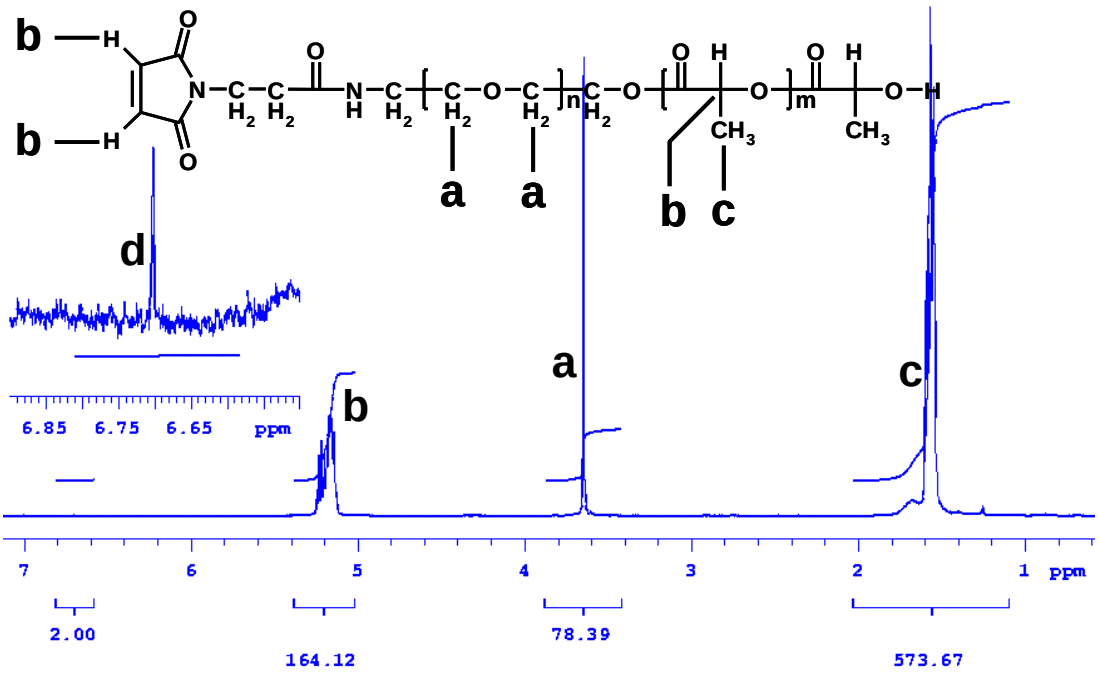


**Figure 7:** 1H-NMR spectrum of maleimide-PEG-PLA block copolymer.

## **APPENDIX 2:** Method for ligand quantification

Method for ligand quantification (Acid hydrolysis and OPA amino acid quantification)
See Pierce reference; Cat# 26025 and 24304 for more detailed instructions on acid hydrolysis and use of *o*-Phthaldialdehyde (OPA) reagent.

In brief and as reported on quarterly report 12, the MAL amount was varied at three levels (80:20; 90:10; 96:4 – w/w) by mixing different proportions of the function copolymer with unmodified PLGA polymer. A 10-fold excess of $(Asp)_4$ peptide ligand was reduced and incubated with freshly prepared nanoparticles at room temperature overnight. The nanoparticles were separated from unconjugated peptide by ultracentrifugation and the pellet dispersed in 1 ml of DI water. The nanoparticle dispersion was extensively hydrolyzed overnight using constant boiling HCl at 120 °C. After hydrolysis, the resulting solution was neutralized and assayed for released aspartate (Asp) amino acid.

An *o*-Phthaldialdehyde (OPA) assay was used to quantify the amount of amino acids. It has been well established that binding of amino acids to OPA compound causes an increase in intrinsic fluorescence of OPA compound. To quantify the amount of released amino acids we developed a standard calibration curve by incubation varying concentration of Asp amino acid with OPA solution. The representative calibration curve for Asp amino acid quantification is shown below (Figure 1). The fluorescence intensity was normalized for the background fluorescence of OPA compound.

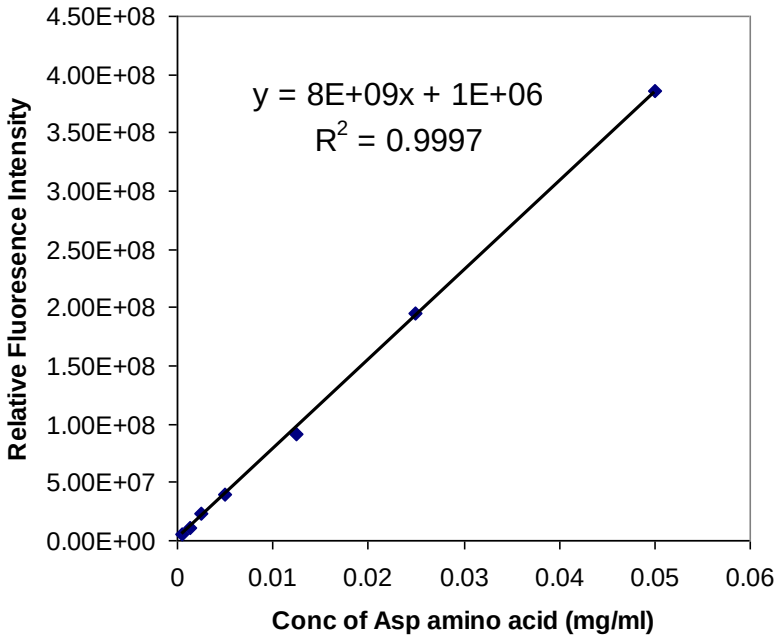


Figure 1. Calibration curve for OPA assay of amino acid content.

Nanoparticles without conjugated $Asp_4$ ligand were used as controls to determine the increase in OPA fluorescence due to any non-specific interaction with polymer fractions. The contribution of control samples was subtracted to determine the effective concentration of hydrolyzed peptide. Figure 2 shows

the resultant concentration of Asp peptide conjugated to nanoparticles at varying levels of MAL concentration in the nanoparticles.

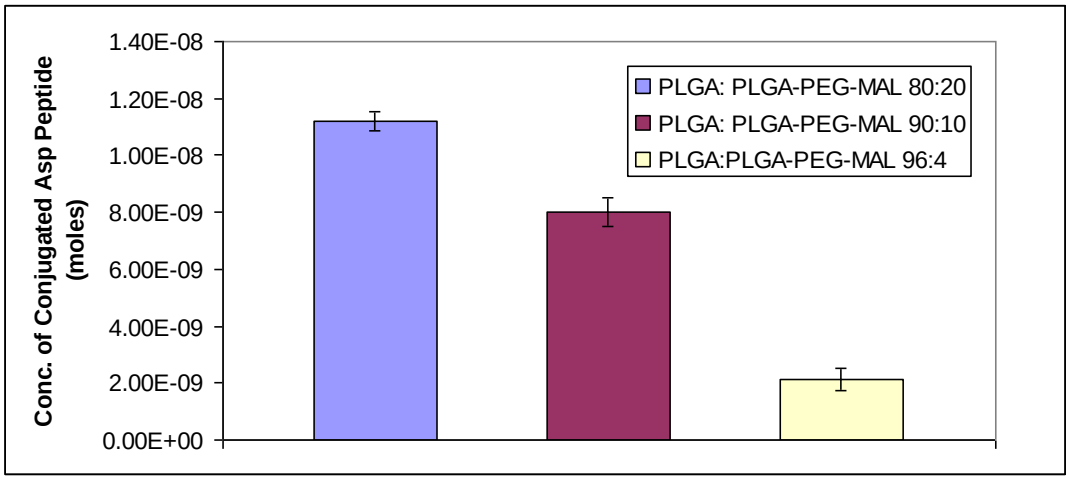


**Figure 2:** Amounts of conjugated $Asp_4$ ligand to nanoparticles containing different compositions of ligand binding sites.

The results show that the amount of conjugated $Asp_4$ ligand follows the availability of MAL functional groups over the given compositional range. The results also highlight that the conjugation efficiency is low. For 80:20 PLGA nanoparticles, the efficiency was approximately 3%. Low conjugation efficiency can be attributed to various factors including accessibility of Mal molecule for conjugation, rapid hydrolysis Maleimide group (~half life of 30-40 minutes), steric hindrance for Asp peptide molecule and possibly a low efficiency in incorporation of polymer chains to form nanoparticles. To obtain a more accurate measure of conjugation efficiency, we would need to determine the concentration of nanoparticles formed using the above approach.

## **Appendix 3:** Development of Bone-Targeting Nanoparticles for Bone Cancer Therapies

**Controlled Release Society: July 7–11, 2007 Long Beach Convention Center Long Beach, California U.S.A. Development and Characterization of Bone-Targeting Nanoparticles S Crumlett, G Rossini, J Trevino, N Vail Southwest Research Institute, USA (Nanoencapsulation section, #156)**

**Development of Bone-Targeting Nanoparticles for Bone Cancer Therapies**

Stefanie Crumlett, Gianny Rossini, M.S., Jack Trevino, Neal K. Vail, Ph.D.
Southwest Research Institute, San Antonio, Texas.

**Statement of Purpose:** We hypothesize that bone-targeting nanocarriers can preferentially accumulate in the skeleton and locally release proteasome inhibitors (PI) to impair the capacity of myeloma cells to survive and grow in vivo, thereby reducing the formation and growth of tumor-induced lytic bone lesions. PIs are not selective to bone and their therapeutic-toxic window may be narrow when administered systemically. Targeted bone delivery has potential to reduce systemic exposure, increase efficacy in the bone environment, and the opportunity to reverse catastrophic disease processes. Site-specific targeting requires quantitatively distinct receptors. We selected the calcified matrix as our initial site for bone-targeting. We identified bone-binding ligands and selected two well-known for their predilection to bone surfaces, methylene bisphosphonate (MBP)[1] and an aspartic acid oligopeptide ($Asp_n$)[2]. We present work on the development and characterization of bone-targeting nanoparticles to be used in our preclinical studies.

**Methods:** Polylactide-co-glycolide (PLGA, 75/25, Brookwood) was used to prepare nanoparticles. Functional polyethylene glycols (PEG) were obtained from NOF Corp. $Asp_4$ was obtained from Sigma. PLGA-b-PEG was prepared by conjugating PLGA to an amine-terminated mPEG via DCC/NHS coupling. Maleimide-terminated PEG-b-PLA copolymer was prepared by ring-opening polymerization of lactide on to a hydroxyl-terminated bifunctional PEG. Maleimide was added to the PEG terminus by reaction with 3-maleimidopropionic acid NHS ester. Amino-MBP was synthesized by modified reported method [3]. Either aMBP or $Asp_n$ was linked via sulfhydryl-amino conversion to the functionalized copolymer. Ligand conjugation was monitored by sulhydryl. All structures were confirmed by $^1$H-NMR. Nanoparticles were prepared by either emulsification/solvent-loss or nanoprecipitation. Solvent was removed by evaporation. Particles were purified by ultracentrifugation or cross-flow filtration and lyophilized. Various lyoprotectants were studied. Particle size was determined by photon correlation spectroscopy and zeta-potential measured at pH 7.4. Preferential binding of ligand-containing nanoparticles to hydroxyapatite substrates was determined using radio-labeled nanoparticles. Model PIs were encapsulated and their release profiles determine *in vitro*.

**Results/Discussion:** In previous work, we prepared ligand-containing liposomes and showed these nanocapsules preferentially adhered to hydroxyapatite substrates in vitro [4]. However, encapsulating hydrophobic actives in liposomes is problematic. Therefore, we turned to polymer nanoparticles as an alternative. Nanoparticles were prepared from PLGA/PLA-PEG blends. Nanoparticles prepared by emulsification ranged in size from 150nm to about 200nm, depending on the PEG content, with particle size decreasing with increasing PEG content. Similarly, zeta-potential decreased with increasing PEG content, suggesting shielding of the PLGA surface by the surface PEG groups, although nanoparticle dispersion stability was not affected. Nanoparticles prepared by nanoprecipitation ranged in size from about 75nm to about 150nm, depending on solvent choice, polymer concentration, and PEG content. Lyophilization of nanoparticle dispersions resulted in irreversible agglomeration. Traditional

lyoprotectants, such as oligosaccharides, reduced agglomeration, but only at concentrations of 0.5% or higher. Pluronic F68 provided excellent lyostability at considerably lower concentrations.

Structural analysis of the custom synthesized maleimide-PEG-b-PLA polymer indicated the PLA segment had a length of about 710 units, or a $M_w$ of about 50k. Attachment of the maleimide group had a conversion of 100% and ligand attachment to the maleimide was similarly determined to occur with high conversion. Ligated polymers were incorporated into PLGA nanoparticles during preparation in compositions up to about 10% wt. The gamma emitter, $^{99m}$Tc, was encapsulated into nanoparticles with efficiency typically of about 20% for radio-labeling. The preferential adherence of these ligand-containing, radio-labeled nanoparticles was evaluated with several hydroxyapatite powders. Attachment of ligand-containing nanoparticles was found to occur in a Langmuir-like behavior. Nanoparticles without targeting ligands had no significant affinity for the HAp substrates.

Proteasome inhibitors PS-1, PS-IX, and MG262 were encapsulated into nanoparticle formulations with encapsulation efficiencies up to about 50%, resulting in payload compositions of typically less than about 10% wt. Particles and payload remained stable through lyoprotection. In vitro release studies showed the actives to be completely released within 1 – 3 weeks.

**Conclusions:** We prepared and verified the structure of bone-targeting ligands conjugated to biodegradable polymers and their use in the formation of polymer nanoparticles. These nanoparticles could be made lyostable with Pluronic F68 being effective at lower, reasonable concentrations than oligosaccharides. We further showed that specifically formulated bone-targeting nanoparticles preferentially adhere to bone-like surfaces. Cancer drugs could be encapsulated in these nanoparticles with reasonable efficiencies and payloads, and further released under in vitro conditions.

**References:** 1. Davis, et al., Semin Nucl Med. 1976; 6:19-31. 2. Kasugai, et al., J Bone Miner Res. 2000; 15:936-943. 3. Kontoci, et al. Synth Comm. 1996; 26:2037-2043. 4. Vail, et al., CRS, 2003.

Abstract presented in Army Health Research Forum (August 31-September 3, 2009 Kansas S9-2 and P25-3 City, MO.

## BONE-TARGETING NANOPARTICLES FOR TREATMENT OF MYELOMA

**Gianny Rossini**

Southwest Research Institute

**Background:** Multiple myeloma is the second most common adult hematologic malignancy and is unique in its propensity to cause bone destruction [Mundy, 1988]. The disease accounts for 1–2% of cancer-related deaths (Jemal, 2003), with 80% of patients suffering devastating and progressive bone destruction. Beneficial effects of conventional therapeutic regimens are modest and relapse is invariable, and therefore, new treatment strategies are of urgent and vital importance.

**Purpose:** The purpose of our work is to determine, in preclinical studies, the potential of skeletally targeted PIs as an efficacious and selective treatment for myeloma. The program hypothesis is that bone-targeting nanocarriers can preferentially accumulate in the skeleton and locally release PIs to impair the capacity of myeloma cells to survive and grow in vivo, thereby reducing the formation and growth of tumor-induced lytic bone lesions.

**Methods:** Site-specific targeting requires quantitatively distinct receptors. We selected the calcified matrix as our initial site for bone-targeting. We identified bone-binding ligands and selected two well-known for their predilection to bone surfaces, methylene bisphosphonate (MBP) (e.g., Davis, 1976) and an aspartic acid oligopeptide (Asp4) (e.g., Kasugai, 2000). We synthesized amino-MBP and confirmed structure by 1H-NMR. Either aMBP or Asp4 was linked via sulfhydryl-amino conversion to a maleimide-functionalized PEG-b-PLA copolymer. Ligand conjugation was monitored by sulhydryl content using UV-Vis spectroscopy. The PEG-b-PLA copolymer was prepared by ring-opening polymerization of lactide in the presence of a hydroxyl-terminated bifunctional PEG. The block copolymer composition was confirmed by 1H-NMR.

**Results:** We prepared nanoparticles with different compositions ratios of PLGA/PLA-b-PEG using the coacervation method and emulsion method with particle size from 100 nm to about 200 nm, depending on the PEG content. Two approaches were used to prepare targeted NPs. For the first approach, polymer was synthesized with ligand already on (PLGA-PEG-ASP4) and particles would form after. For the second approach, ligand was conjugated after particle formation. The benefit of the first method is reproducibility and speed of processing. Cryoprotectants, such as disaccharides, were required to avoid particle agglomeration during lyophilization. The selected bone-targeting ligands were conjugated to the surfaces of functionalized nanoparticles. Adherence of these ligand-containing nanoparticles to hydroxyapatite substrates was confirmed by radiolabeling particles with Tc99m. Cell base assay confirmed the activity of encapsulated drug. Early biodistribution of non-targeted NP shows prolonged blood circulation times with a half-life of around 4 hours.

**Conclusion:** We demonstrated the formulation and characterization of nanoparticles for bone-targeting. We showed that these specifically formulated bone-targeting nanoparticles preferentially adhere to bone-like surfaces in vitro. In vivo biodistribution of two untargeted nanoparticles' formulation demonstrates prolonged circulation times; and the encapsulated FDA-approved drug Velcade is fully active. This positions us to proceed with in vivo work to study the biodistribution and efficacy of these nanoparticles. This technology has tremendous potential in the treatment of myeloma and other musculoskeletal diseases and disorders.

---

*This work was supported by the U.S. Army Medical Research and Materiel Command under W81XWH-05-C-0004.*

Transactions Vol. 35, New Orleans, LA, 20100399 - Bone-targeting Nanoparticles: Synthesis, Biodistribution and In-vitro Efficacy Cheng, Xingguo; Rossini, Gianny Bioactive Biomaterials; Tumors; Orthopaedic Pathology

# Bone-targeting Nanoparticles: Synthesis, Biodistribution and *In-vitro* Efficacy

[1]Rossini G; +[1]Cheng X;
+[1]Southwest Research Institute, San Antonio, TX
xcheng@swri.org

## INTRODUCTION:

Bone is a composite matrix of organic collagen and inorganic apatite constituents that could potentially serve as site-specific receptors for targeted-delivery vehicles[1]. Small molecules such as bisphosphonates (BP)[2]or aspartic acid (Asp) oligopeptide[3] had been shown able to target bone *in vitro* and *in vivo*. Targeted drug delivery system has the benefits of lower side effect, lower systemic toxicity, lower dosage requirement and increased efficacy. In current study, we aim to develop a bone-targeted drug delivery system which carries proteosome inhibitors to treat myeloma cancer[4].

## METHODS:

Synthesis of bone targeting nanoparticles: PLGA-PEG polymers was modified to have bisphosphonate or $(Asp)_6$ end groups. A water-oil-water double emulsion method was used to synthesize nanoparticles. Briefly, 100 mg of PLGA and PLGA-PEG polymer (modified or unmodified) were dissolved in 6mL methylene chloride. Drug was incorporated in 100-200μL water phase and emulsified in the above solution, which was further dispersed in 1% sodium cholate solution. This double emulsion solution was diluted in 0.5 % sodium cholate solution and evaporated for 2 hrs to remove the solvent. The nanoparticles were collected by ultracentrifuge at 20,000 rpm. For radio labeling of nanoparticles, BSA-Tc[99] conjugate, or fresh Tc or oxidized Tc was introduced in the water phase and similar nanoparticles synthesis procedure as above was followed.

In vitro binding with hydroxyapatite: Binding of nanoparticles with hydroxyapatite was quantified by two independent method: in one method the intensity of radioactive Tc was used to quantify the binding efficiency. In another method, the nanoparticles were modified with a pyrene moiety during synthesis and the binding was quantified by a fluorescence intensity reading.

Biodistribution in mouse: Radiolabeled NPs was injected into the mouse tail vein and imaged was taken by μSPECT and μCT.

Drug release and In vitro efficacy against myeloma cancer cells: 50mg of NPs was suspended 2mL PBS solution at 37 °C at shaking speed of 1 Hz. At each time point the released drug was collected and fresh new PBS was added. Murine 5TGM1 myeloma cells were seeded at 5,000 cells per well in 96-well plates in 100μl media per well. Then free drug, released bortezomib from nanoparticles, and drug-loaded NPs were then added at 50 μL/well at 1:3 dilution after 24 hrs. After incubation the cells with the above drugs or NP for 72 hrs, 15 μl of MTT solution was added to each well and the viability of cells was analyzed. The absorbance of MTT solution at 570 nm correlates with the number of viable cells after 72 hrs' drug or nanoparticles exposure. Because velcade will lose some activity after exposure to light, all experiment procedures were done in the dark or yellow light.

## RESULTS:

Depending on the composition of PLGA and PLGA-PEG, the size of nanoparticles was around 100-200 nm (Figure 1A). Three methods had been used to load $^{99m}$Tc inside nanoparticles. Highest Tc loading was achieved by using Bovine Serum Albumin (BSA)-Tc conjugates (Figure 1B).

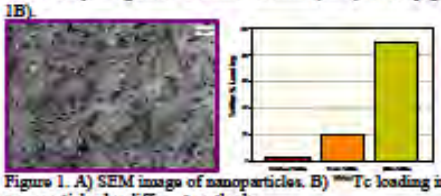

Figure 1. A) SEM image of nanoparticles. B) $^{99m}$Tc loading inside nanoparticles by different methods.

The binding efficiency of untargeted nanoparticles to HA was around less than 20%. For both BP and $(Asp)_6$ conjugated particles, the binding efficiency increased as the amount of HA used increased. It seems that BP ligand is much more effective in binding with HA than $(Asp)_6$ ligand

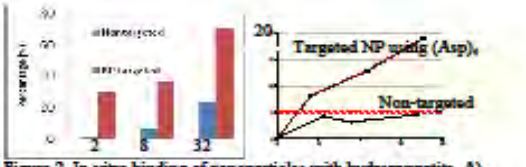


Figure 2. In-vitro binding of nanoparticles with hydroxyapatite. A) Targeted NPs with BP ligand bind more than non-targeted NPs. B) Targeted NPs with $(Asp)_6$ ligand bind more than non-targeted NPs as quantified by fluorescence assay.

Liver (22-36%) and spleen (3-58%) had the most uptake of NPs in the non-bone organs (Figure 3A). Bone had an uptake of around 2-9.8%. For mouse with myeloma cancer, the targeted NPs had significantly more binding to skeletal tissue than non-targeted NPs (Figure 3B).

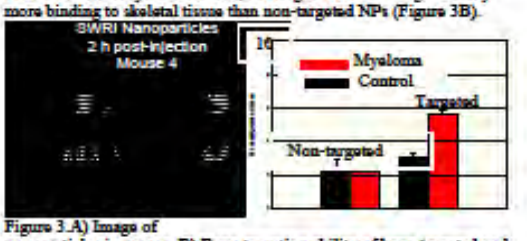


Figure 3.A) Image of nanoparticles in mouse. B) Bone targeting ability of bone targeted and non-targeted NPs in healthy and diseased animals with myeloma cancer.

Velcade can be gradually released followed by a burst release (Figure 4A). The *in vitro* Cytotoxicity test indicates that released drug from NPs has same efficacy as free drug (P>0.05, 4.5±0.8 v.s. 3.86 ±1.76 nM ). NPs directly added to murine 5TGM1 myeloma cells has slightly higher IC50 value than free drug (P>0.05, 7.59 ±1.5 v.s. 3.86 ±1.76). However, statistical analysis indicate there is no significant difference between all three groups (Figure 4B)

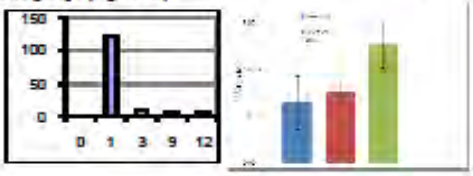


## DISCUSSION:

We prepared bone-targeted nanoparticles which can load drugs inside. In vitro and in vivo binding and biodistribution studies indicated that nanoparticles preferably bind to hydroxyapatite surface. For diseased mouse, targeted NPs show significantly higher binding to bone than Non-targeted NPs. Non-targeted NPs have a circulation time around 4 hours. Efficiency study indicated the both the released drug and the nanoparticles are effective to kill the myeloma cancer cells in vitro. In vivo study of the efficacy of bone targeted NP for treatment of myeloma cancer is underway.

## REFERENCES:

1. Olszta, M.J., et al., Materials Science & Engineering R-Reports, 2007. 58(3-5): p. 77-116.
2. Page, P.C.B., et al.,Tetrahedron, 2001. 57(9): p. 1837-1847.
3. Wang, D., et al., Bioconjugate Chemistry, 2003. 14(5): p. 853-859.
4. Terpos, E., M. Roussou, and M.A. Dimopoulos, Expert Opinion on Drug Metabolism & Toxicology, 2008. 4(5): p. 639-654.

**Appendix 4:** Targeted Therapies of Myeloma and Metastatic Bone Cancer Final Report Efficacy Study

SwRI Subcontract No. B99044X **FINAL REPORT** Babatunde Oyajobi, MD, PhD

**"Targeted Therapies of Myeloma and Metastatic Bone Cancer" (W81XWH05C004)**

**UTHSCSA Sub-contract PI: Babatunde O. Oyajobi, M.D., Ph.D.**

**Scientific Report**

Sub-contract B99044X was signed on March 30, 2010 with an effective start date of March 1, 2010.

**PREAMBLE:**

1. We obtained approval for the UTHSCSA IACUC protocol (# 05128-34-04-A, C) through 09/30/10 and to transferred the protocol from Dr. Garrett to Dr. Oyajobi as PI.
2. We obtained approval of the IACUC protocol by the USAMRMC ACURO.
3. We ordered C57BL/KaLwRijHsd mice from Harlan, The Netherlands and we were notified about two weeks ago that delivery date will be February 2011. As this delivery schedule will not work, following consultation with grant PI at SwRI, Gianny Rossini, we decided to substitute *bg-nu-xid* mice for the C57BL mice.
4. We have since obtained additional approval for the substitution from the UTHSCSA IACUC and subsequently the USAMRMC ACURO. The *bg-nu-xid* mice were ordered from Harlan immediately after ACURO approval was obtained we were notified on 6/29/10 that delivery would be on 07/08/10.
5. *bg-nu-xid* mice were delivered as scheduled on 07/08/10 (APPENDIX A) and the in vivo study commenced on Tuesday 07/13/10 as agreed with grant PI at SwRI and according to agreed experimental protocol (APPENDIX B). The minor delay in starting was due to unforeseen SwRI-related issues (see emails from PI, Gianny Rossini; APPENDIX A). SWRI provided two different types of technetium-99m ($Tc^{99m}$)-labeled nanoparticles (NP *Targeted* and *Non-targeted*; each administered at two different does – 0.2 and 1.0mg/kg body weight), which were injected intravenously as soon as they were delivered to UTHSCSA personnel. Tumor-bearing mice treated with Velcade™ (also administered at 0.2 and 1.0mg/kg body weight) served as treatment controls since we had previously reported that Velcade™ has a potent anti-tumor effect in myeloma-bearing mice (4). Experiment was terminated after 28 days and half of each group (determined randomly) were sacrificed on day 28 (08/10/10) and the other half was sacrificed the following day (08/11/10). This was due to the very large number of mice and the consequent volume of work that made it impossible to accomplish everything in one day.

**EXPERIMENTAL GROUPS**

| | | Mouse ID code# |
|---|---|---|
| I: | Control (Non tumor-bearing) | 1-6 |
| II: | Vehicle | 7-14 |
| III: | NP Vehicle | 15-22 |
| IV: | Velcade 0.2mg/kg body weight | 23-30 |
| V: | Velcade 1mg/kg body weight | 31-38 |
| VI: | NP 0.2mg/kg body weight (*Non-targeted*) | 39-46 |
| VII: | NP 1mg/kg body weight (*Non-targeted*) | 47-54 |
| VIII: | NP 0.2mg/kg body weight (*Targeted*) | 55-62 |
| IX: | NP 1mg/kg body weight (*Targeted*) | 63-70 |

Note: All groups *except* group I are tumor-bearing

1

**RESULTS AND DISCUSSION:**

- **Clinical parameters for each mouse: weight loss, presence of paraparesis/paraplegia**
  (a) Data for body weight (g) and graphs are presented in APPENDIX C (Excel; Sheet 1)
  All groups gained weight steadily until the last week when all tumor-bearing groups (II-IX) lost weight (~10%). The extent of weight loss was not significantly different in any of the tumor bearing groups (ANOVA). The control (sham) group that received only PBS through the tail vein (no tumor cells), continued to gain weight through the last week of the experiment as would be expected. Based on these data, it is reasonable to conclude that there is no overt toxic effect of any of the four nanoparticles
  (b) Three (mice ID code #30, 48,53) were found dead having died spontaneously (cause unknown) overnight before the end of the scheduled experiment; they had not been previously observed to be sick or either paraparetic or paraplegic. Because *rigor mortis* had set in and it was impossible to draw blood for preparing sera, these mice were excluded from further analysis. One mouse developed paraplegia late on day 27, one day before scheduled termination of experiment (ID code #18) and three more were found paraplegic on day 28, the scheduled termination study (ID code# 43,62,67). All three mice were included in the cohort sacrificed on 08/10/10. There does not appear to be any association between development of paraplegia and the treatment administered; development of paraplegia was random and probably related to tumor exiting the vertebrae and infiltrating the spinal cord. Summary of this is presented in APPENDIX C (BodyWeight.xlsx; Sheet 2).

- **Serum monoclonal IgG2bκ titers**- (used as a surrogate for overall tumor load)
  All myelomas (human or murine) are unique in that each is a clone producing a specific monoclonal paraprotein, which in the case of the 5TGM1 myeloma is an IgG2bκ (1,3). Our group and others have shown serum titers of the 5TGM1 monoclonal paraprotein, measured by a sandwich ELISA, to be a reliable surrogate for and correlate with overall myeloma tumor load (1,2,4-8). We determined the titers in serum obtained at baseline (07/12/10; day -1) and immediately prior to sacrifice (08/10/10; day 28) and these data are presented in FIGURE 1 and APPENDIX D (IgG2b.xlsx; Sheet 1). To determine if there were significant differences between groups, ANOVA (with post-hoc correction by Fisher PLSD test) was performed using StatView program with significance levels set at 0.1, 1 and 5% (corresponding to $p<0.001$, $p<0.01$, $p<0.05$ respectively) (APPENDIX E).

  Summary:
  (*i*) For both vehicles (groups (I & II), serum IgG2bκ titers were significantly elevated at sacrifice (average fold change/group >3,000-fold) compared to base-line values.
  (*ii*) Velcade (internal treatment control) was effective in reducing tumor burden; tumor load on both Velcade groups (IV & V) were significantly reduced compared to vehicle control (group II) ($p<0.001$)
  (*iii*) Both NP (*Targeted*, groups VI & VII) and NP (*Non-targeted*; groups VIII & IX) also exhibited potent anti-myeloma effect reducing tumor load in mice at both doses tested significantly compared to NP vehicle (group III) ($p<0.001$)
  (*iv*) Unlike the Velcade-treated groups, where there was a dose-relationship in the anti-tumor effect (IgG2bκ; $p<0.01$, group IV vs group V), neither NP (*Targeted*) nor NP (*Non-targeted*) exhibited a similar dose-dependency; serum IgG2bκ titers were not significantly different between the higher (1.0mg/kg body weight) dose and the lower (0.2mg/kg body weight dose) for either type

of NP. The reason for this is unclear and without data on the pharmacokinetic and pharmacodynamic properties of the NPs, as well as the amount of NPs reaching bone and the rate of release locally in bone, any conclusions will be highly speculative at best.

(v) Compared to the equivalent dose of Velcade, only with the NP (*Non-targeted*) at 0.2mg/kg was tumor burden significantly reduced and this was just barely (p=0.0499). There was no statistically significant difference between NP (*Targeted*) and NP (*Non-targeted*) at either dose tested. Again, it is unclear why there is no difference between the two classes of NPs: *Targeted* and *Non-targeted*, and without more data any conclusions would be speculative.

- Whole-body GFP scans
  Whole body optical fluorescence scans (8) were performed according to protocol. After mice were euthanized, the whole skeleton and viscera (organs) were laid out and re-imaged. All images were captured and saved as high-resolution TIFF files on a Mac computer. A summary of the gross observations (fluorescent foci) at necropsy (as visualized on the computer screen) are collated and presented in APPENDIX F and TIFF files are provided on a CD. Please note that the data in the Excel spreadsheet is only to indicate whether there is fluorescence in a particular organ/tissue or not and does not signify the extent and brightness of the fluorescence.
  The excised spleens were also weighed whole as splenomegaly is not uncommon in this model due to the fact that the spleen is a hematopoietic organ in the mouse and myeloma tumors engraft in this organ in most animal models of myeloma. Splenic wet weight data are also included in APPENDIX F. As we had previously reported (8), in the Velcade 1mg-treated group the incidence of splenomegaly was markedly reduced with only 3 out of 8 mice having enlarged spleens and even then these were only very moderately enlarged (0.2-0.3g versus normal wet weight $\leq$ 0.1g). Surprisingly, there was no effect of either class of NP at either dose tested on reducing splenic enlargement. Even in the NP *Targeted* 1mg-treated group 7 out of 8 had splenomegaly and these were all massive ($\geq$0.9g). This situation was similar in the NP *Non-targeted* 1mg-treated group where all 6 mice surviving at the end of the experiment had similarly enlarged spleens ($\geq$0.7g). The reason why the NP-treated mice did not exhibit any reduction in spleen size as would be expected given the significant reductions in monoclonal paraprotein titers is unclear. *On possibility, albeit entirely speculative, is that there are one or more molecules(s) in the circulation in NP-treated mice that is masking the detection of the paraprotein in the sandwich ELISA.*

**CONCLUSION:**

- Both classes of NPs tested exhibit anti-tumor efficacy in the murine 5TGM1 model of multiple myeloma.

01/28/11

Babatunde O. Oyajobi
*Associate Professor of Cellular & Structural Biology and Medicine*

Date

**FIGURE 1: Serum IgG2bκ levels at sacrifice**

Top panel: mean ± SEM; Bottom panel: *Box plot* of values (circles represent values outside 95% confidence limit

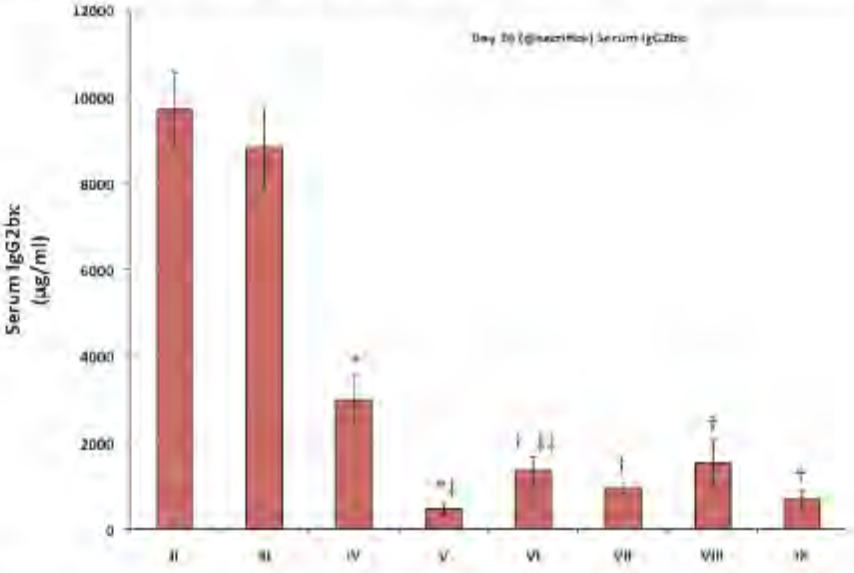


* $p<0.001$, vs Vehicle (Grp II)

† $p<0.001$, vs NP Vehicle (Grp III)

‡ $p<0.01$, vs lower dose of same compound (Grp IV)

‡‡ $p<0.05$, vs same dose of Velcade (Grp IV)

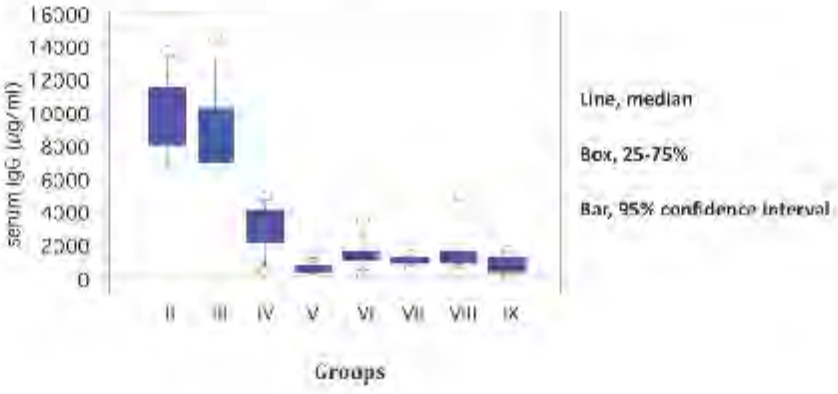

**References**


1. Dallas SL, Garrett IR, Oyajobi BO, Dallas MR, Boyce BF, Bauss F, Radl J, Mundy GR. Ibandronate reduces osteolytic lesions but not tumor burden in a murine model of myeloma bone disease. *Blood* 1999 Mar;93(5):1697-1706.
2. Edwards CM, Edwards JR, Lwin ST, Esparza J, Oyajobi BO, McCluskey B, Munoz S, Grubbs B, Mundy GR. Increasing Wnt signaling in the bone marrow microenvironment inhibits the development of myeloma bone disease and reduces tumor burden in vivo. *Blood* 2008 Mar;111(5):2833-2842.
3. Garrett IR, Dallas S, Radl J, Mundy GR. A murine model of myeloma bone disease. *Bone* 1997 Jun;20(6):515-20.
4. Goel A, Dispenzieri A, Geyer SM, Greiner S, Peng KW, Russell SJ. Synergistic activity of the proteasome inhibitor PS-341 with non-myeloablative $^{153}$Sm-EDTMP skeletally targeted radiotherapy in an orthotopic model of multiple myeloma.. *Blood* 2006 May;107(10):4063-70.
5. Murillo O, Arina A, Hervás-Stubbs S, Gupta A, McCluskey B, Dubrot J, Asís Palazón A, Alpiliketa A, Alfaro C, Solano S, Perez-Gracia JL, Oyajobi BO, Melero I. Therapeutic efficacy of anti-CD137 agonistic mAb in mouse models of myeloma. *Clinical Cancer Research* 2008 Nov;14(21):6895-906.
6. Olson DL, Buckly LC, Leone DR, Dolinski BM, Lobb RR. Anti-alpha4 integrin monoclonal antibody inhibits multiple myeloma growth in a murine model. *Molecular Cancer Therapeutics* 2005 Jan;4(1):91-9.
7. Oyajobi BO, Franchin G, Williams PJ, Pulkrabek D, Gupta A, Munoz S, Zhao M, Chen D, Sherry BA, Mundy GR. Dual effects of macrophage inflammatory protein-1alpha on osteolysis and tumor burden in the murine 5TGM1 model of myeloma bone disease. *Blood* 2003 Jul;102(1):311-319.
8. Oyajobi BO, Munoz S, Kakonen R, Williams PJ, Gupta A, Story B, Grubbs B, Armstrong A, Dougall WC, Garrett IR, Mundy GR. Detection of myeloma tumors in skeleton of live mice by whole body optical fluorescence imaging. *Molecular Cancer Therapeutics* 2007 Jun;6(6):1701-1708.
9. Wang S, Yang J, Qian J, Wezeman M, Kwak LW, Yi Q. Tumor evasion of the immune system: inhibiting p38 MAPK signaling restores the function of dendritic cells in multiple myeloma. *Blood* 2006 Mar;107(6):2432-9.

## **Appendix 5:** *In-vivo* efficacy

From: Gianny Rossini <gianny.rossini@swri.org>
Subject: NPs
Date: July 9, 2010 11:02:57 AM CDT
To: "Oyajobi, Babatunde" <OYAJOBI@uthscsa.edu>
Cc: 'Gloria Gutierrez' <gloria.gutierrez@swri.org>

**Kay:**
**As we discussed over the phone today, we will prepare the NP for injection every Tuesday staring the next Tuesday July 13. NP will be made fresh every Tuesday and be ready for injection on afternoon around 2-4 PM). NP will be made for the next 3 or 4 weeks as needed to complete the study. We will provide NP vehicle and NP-velcade formulation to inject in a volume enough for 100ul per animal using the i.v tail injection protocol for a total of 8 animals per group and some extra volume for spare, NP will be re-suspended in saline. As I said before, I think we can use 0.2 and 1 .0 mg/kg doses instead of the 3 doses originally proposed on the SOW (0.1;0.5 and 1mg/k). The main reason is to make space for targeted and non targeted NP and the corresponding controls. Comments and suggestions are welcome,**

**Group 1; vehicle**
**Group 2; NP vehicle**
**Group 3; Velcade 0.2mg/kg**
**Group 4; Velcade 1 mg/kg**
**Group 5; NP 0.2mg/kg (non targeted)**
**Group 6; NP 1mg/kg (non targeted)**
**Group 7; NP 0.2mg/kg (targeted )**
**Group 8; NP 1 mg/kg (targeted )**

**Thanks,**
**Gianny**

Gianny Rossini
Sr Research Scientist
Biochemistry & Biomaterials Group Leader
Tel: (210) 522-6347
Fax: (210) 522-4565
Southwest Research Institute
San Antonio TX 78238

From: Gianny Rossini <gianny.rossini@swri.org>
Subject: NPs
Date: July 7, 2010 11:25:33 AM CDT
To: "Oyajobi, Babatunde" <OYAJOBI@uthscsa.edu>
Cc: 'Gloria Estela Gutierrez' <gloria.gutierrez@swri.org>, 'Sapna Desai' <sapna.desai@swri.org>

Hi Kay,
We need to talk about the upcoming animal study, please let me know at time and date that would fit you. I have to say that July 9 and July 12 are difficult days for us and we should avoid those days for this study. Otherwise any other day should be fine, all we need from you is a date for injection and we will prepare the NP in 100ul on saline for iv injection. About the animal groups, we need to drop the 0.1 dose and replace that for more nanoparticles groups as follow.

Group 1; vehicle
Group 2; NP vehicle
Group 3; Velcade 0.5mg/kg
Group 4; Velcade 1 mg/kg
Group 5; NP 0.5mg/kg (non targeted)
Group 6; NP 1mg/kg (non targeted)
Group 7; NP 0.5mg/kg (targeted )
Group 8; NP 1 mg/kg (targeted )

Thanks
Gianny

Gianny Rossini
Sr Research Scientist
Biochemistry & Biomaterials Group Leader
Tel: (210) 522-6347
Fax: (210) 522-4565
Southwest Research Institute
San Antonio TX 78238

**Appendix 6:** Murine STGM1-GFP myeloma cells inoculated in Tumor-Bearing Groups Report

**APPENDIX B**

**Murine 5TGM1-GFP myeloma cells inoculated in TUMOR-BEARING GROUPS (II-IX)**

| | ID (code) | Route of admin | #cells inoculated i.v./100µl PBS |
|---|---|---|---|
| I: Control | 1-6 | IV (sham) | No cells/PBS only |
| II: Vehicle | 7-14 | IV | $10^6$ |
| III: NP Vehicle | 15-22 | IV | $10^6$ |
| IV: Velcade 0.2mg/kg | 23-30 | IV | $10^6$ |
| V: Velcade 1mg/kg | 31-38 | IV | $10^6$ |
| VI: NP 0.2mg/kg (non-targeted) | 39-46 | IV | $10^6$ |
| VII: NP 1mg/kg (non-targeted) | 47-54 | IV | $10^6$ |
| VIII: NP 0.2mg/kg (targeted) | 55-62 | IV | $10^6$ |
| IX: NP 1mg/kg (targeted) | 63-70 | IV | $10^6$ |

**Age/Strain/Species tested:** 5-6 week old female naïve *bg-nu-xid* mice (*nu/nu* (n=70) – from Harlan, Indianapolis, IN; delivered 07/08/10

**Tumor Cell Inoculation:** Inoculate cells via intravenous route through tail vein @ $1x10^6$ cells in 0.1ml PBS/mouse on 07/13/10 (Day 0)

**Route of Administration of Test Compounds:** Nanoparticles (NP) - intravenous tail vein injection; Velcade™ (Bortezomib) – intraperitoneal injection
Using BD Ultra fine insulin syringe w/ 31G needle

**Dose interval and duration of dosing:** Once a week; starting 07/13/10 (day 0; Tuesday), and then weekly thereafter for 4 weeks (total 4 doses). Test compounds will be delivered by SwRI personnel and injected immediately

**Methodology:** Weigh animals, randomize into groups and code (ID) before experiment starts, so that all groups have approximately the same mean body weights at start. For tumor bearing groups (II-IX), intravenous inoculation of cells will be random. Observe animals carefully (daily from start through week 3 and twice daily thereafter) for any abnormalities. Record body weights weekly.

**Body Weights:** Take body weights every Monday starting w/ baseline on 07/12/10 (day -1).

**Serum collection:** Collect serum using retro orbital bleeding method at baseline (07/12/10; day -1) and weekly (Mondays) thereafter, and on the day of sacrifice using intra-cardiac bleeding method.

**Radiographic and Optical fluorescence imaging:** Obtain whole body X-rays on days 14 and 28; whole body GFP scans on days 14, 21 and 28 post-tumor cell inoculation.

**Sacrifice Day:** (*i*) When animals develop paraplegia/paraparesis either on/or before day 28 which ever comes first; (*ii*) if any mouse loses >10% of body weight in one week (vs the preceding week's weight)

**Tissue harvesting:** After the last set of whole body X-rays, GFP scans and serum collection, euthanize mice. Immediately harvest all skeletal tissues and then viscera (brain, kidneys, spleen, liver, heart and lungs). After tissue harvesting, scan all tissues again before transferring to cold 4% paraformaldehyde for fixation.

## **Appendix 7:** Body Weights

| | | ID (Code) | Date | Day post-tumor cell inoculation |
|---|---|---|---|---|
| **Mouse found dead - cause unknown** | | | | |
| Gr. IV | Velcade 0.2mg | 30 | 07/27/10 | 15 |
| Gr. VII | NP 1mg, Non-targeted | 53 | 08/04/10 | 23 |
| Gr. VII | NP 1mg, Non-targeted | 48 | 08/06/10 | 25 |
| **Mouse found paraplegic** | | | | |
| Gr. III | NP Vehicle | 18 | 08/09/10 | 28 |
| Gr. VI | NP 0.2mg, Non-targeted | 43 | 08/10/10 | 29 |
| Gr. VIII | NP 0.2mg, Targeted | 62 | 08/10/10 | 29 |
| Gr. IX | NP 1.0mg, Targeted | 67 | 08/10/10 | 29 |

## **Appendix 8:** IgG2b Levels Raw Data

| | | | | Base line | | | Sacrifice | | |
|---|---|---|---|---|---|---|---|---|---|
| | Baseline | Sac Day | | MEAN | SD | SE | MEAN | SD | SE |
| ID (code) | (µg/ml) | (µg/ml) | FOLD | 3.97 | 2.10 | 0.74 | 9693.22 | 2441.16 | 863.21 |
| Group II- Vehicle | | | | | | | | | |
| 7 | 4.74 | 8831.80 | 1862 | | | | | | |
| 8 | 3.36 | 6935.20 | 2064 | | | | | | |
| 9 | 7.98 | 12452.00 | 1560 | | | | | | |
| 10 | 5.29 | 10211.35 | 1929 | | | | | | |
| 11 | 1.58 | 9724.40 | 6137 | | | | | | |
| 12 | 2.30 | 13564.65 | 5891 | | | | | | |
| 13 | 4.40 | 9355.55 | 2128 | | | | | | |
| 14 | 2.09 | 6470.80 | 3099 | | | | | | |
| | | | 3084 | | | | | | |
| | | | | | | | | | |
| | | | | | | | | | |
| Group III- NP Vehicle | | | | | | | | | |
| 15 | 3.43 | 6873.30 | 2003 | 2.46 | 1.84 | 0.65 | 8804.54 | 2648.42 | 936.50 |
| 16 | 0.63 | 14430.50 | 22741 | | | | | | |
| 17 | 3.27 | 7830.20 | 2396 | | | | | | |
| 18 | 6.03 | 9938.35 | 1649 | | | | | | |
| 19 | 3.05 | 7464.35 | 2445 | | | | | | |
| 20 | 1.40 | 6792.60 | 4865 | | | | | | |
| 21 | 1.09 | 6893.25 | 6328 | | | | | | |
| 22 | 0.81 | 10213.80 | 12641 | | | | | | |
| | | | 6883 | | | | | | |
| | | | | | | | | | |
| | | | | | | | | | |
| | | | | | | | | | |
| | | | | | | | | | |
| Gr. IV - Velcade 0.2mg | | | | | | | | | |
| 23 | 2.32 | 4779.38 | 2061 | 1.71 | 0.60 | 0.23 | 2968.02 | 1534.17 | 580.03 |
| 24 | 0.80 | 1886.33 | 2367 | | | | | | |
| 25 | 1.62 | 4004.48 | 2475 | | | | | | |
| 26 | 1.33 | 3840.13 | 2880 | | | | | | |
| 27 | 2.10 | 2338.00 | 1114 | | | | | | |
| 28 | 1.35 | 3610.53 | 2665 | | | | | | |
| 29 | 2.46 | 317.29 | 129 | | | | | | |
| 30 | ~~1.33~~ | N/A | N/A | | | | | | |
| | | | 1997 | | | | | | |
| | | | | | | | | | |
| | | | | | | | | | |
| | | | | | | | | | |
| | | | | | | | | | |
| Gr. V - Velcade 1.0mg | | | | | | | | | |
| 31 | 5.21 | 1247.69 | 239 | 1.89 | 1.46 | 0.52 | 446.23 | 375.36 | 132.73 |
| 32 | 2.16 | 126.91 | 59 | | | | | | |
| 33 | 1.22 | 126.91 | 104 | | | | | | |
| 34 | 0.76 | 289.71 | 380 | | | | | | |
| 35 | 0.83 | 288.40 | 348 | | | | | | |
| 36 | 2.39 | 700.00 | 293 | | | | | | |
| 37 | 1.42 | 497.44 | 349 | | | | | | |
| 38 | 1.15 | 292.77 | 255 | | | | | | |
| | | | 253 | | | | | | |
| | | | | | | | | | |
| | | | | | | | | | |
| | | | | | | | | | |
| Gr. VI - NP 0.2mg, non-targeted | | | | | | | | | |
| 39 | 1.84 | 1047.04 | 570 | 2.10 | 1.22 | 0.43 | 1341.23 | 915.28 | 323.65 |
| 40 | 1.62 | 3322.10 | 2052 | | | | | | |
| 41 | 1.57 | 126.91 | 81 | | | | | | |
| 42 | 1.10 | 872.86 | 794 | | | | | | |
| 43 | 1.92 | 1594.86 | 832 | | | | | | |
| 44 | 5.02 | 1044.60 | 208 | | | | | | |
| 45 | 2.12 | 1419.12 | 668 | | | | | | |
| 46 | 1.58 | 1302.36 | 827 | | | | | | |
| | | | 754 | | | | | | |
| | | | | | | | | | |
| | | | | | | | | | |
| | | | | | | | | | |
| | | | | | | | | | |
| | | | | | | | | | |

| | | | | Base line | | | Sacrifice | | |
|---|---|---|---|---|---|---|---|---|---|
| Gr. VII – NP 1.0mg, non-targeted | Baseline | 5ac Day | | MEAN | SD | SE | MEAN | SD | SE |
| 47 | 1.87 | 549.20 | 294 | 1.21 | 0.48 | 0.17 | 929.46 | 279.71 | 114.22 |
| 48 | ~~1.58~~ | N/A | N/A | | | | | | |
| 49 | 1.44 | 1167.04 | 812 | | | | | | |
| 50 | 1.09 | 717.68 | 657 | | | | | | |
| 51 | 1.55 | 1307.88 | 846 | | | | | | |
| 52 | 0.63 | 947.61 | 1493 | | | | | | |
| 53 | ~~0.71~~ | N/A | N/A | | | | | | |
| 54 | 0.66 | 887.36 | 1336 | | | | | | |
| | | | 906 | | | | | | |
| Gr. VIII - NP 0.2mg, targeted | | | | | | | | | |
| 55 | 0.67 | 740.06 | 1105 | 0.67 | 0.07 | 0.02 | 1512.30 | 1491.55 | 527.42 |
| 56 | 0.63 | 1384.40 | 2182 | | | | | | |
| 57 | 0.63 | 963.78 | 1519 | | | | | | |
| 58 | 0.63 | 642.99 | 1013 | | | | | | |
| 59 | 0.63 | 5057.50 | 7970 | | | | | | |
| 60 | 0.63 | 1303.49 | 2054 | | | | | | |
| 61 | 0.67 | 1624.86 | 2427 | | | | | | |
| 62 | 0.83 | 381.33 | 457 | | | | | | |
| | | | 2341 | | | | | | |
| | 0.66 | 199.74 | 303 | 0.81 | 0.33 | 0.12 | 676.95 | 565.65 | 200.02 |
| 64 | 0.63 | 126.91 | 200 | | | | | | |
| 65 | 0.63 | 257.31 | 405 | | | | | | |
| 66 | 0.63 | 398.04 | 627 | | | | | | |
| 67 | 1.18 | 1549.99 | 1312 | | | | | | |
| 68 | 0.63 | 1495.21 | 2356 | | | | | | |
| 69 | 1.47 | 801.95 | 544 | | | | | | |
| 70 | 0.63 | 586.45 | 924 | | | | | | |
| | | | 834 | | | | | | |

| Mean (Baseline) | SD | SE | mean (sacrifice) | SD | SE |
|---|---|---|---|---|---|
| 3.969 | 2.104 | 0.744 | 9693.219 | 2441.165 | 863.212 |
| 2.464 | 1.842 | 0.651 | 8804.544 | 2648.424 | 936.501 |
| 1.664 | 0.576 | 0.204 | 2968.016 | 1534.167 | 580.025 |
| 1.894 | 1.463 | 0.517 | 446.230 | 375.356 | 132.728 |
| 2.096 | 1.220 | 0.431 | 1341.232 | 915.285 | 323.651 |
| 1.191 | 0.482 | 0.170 | 929.462 | 279.713 | 114.215 |
| 0.668 | 0.069 | 0.024 | 1512.301 | 1491.552 | 527.423 |
| 0.811 | 0.329 | 0.116 | 676.950 | 565.651 | 200.018 |

| Average | Baseline | Sac Day |
|---|---|---|
| II | 4.0 | 9693 |
| III | 2.5 | 8805 |
| IV | 1.7 | 2968 |
| V | 1.9 | 446 |
| VI | 2.1 | 1341 |
| VII | 1.2 | 929 |
| VIII | 0.7 | 1512 |
| IX | 0.8 | 677 |

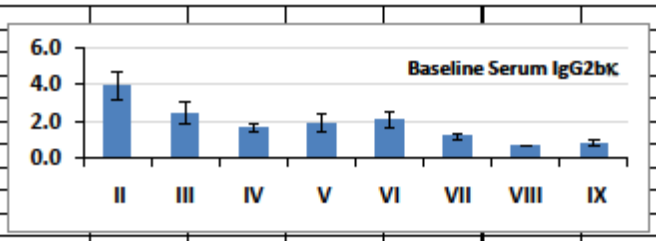


| | Sac Day |
|---|---|
| II | 9693 |
| III | 8805 |
| IV | 2968 |
| V | 446 |
| VI | 1341 |
| VII | 929 |
| VIII | 1512 |
| IX | 677 |

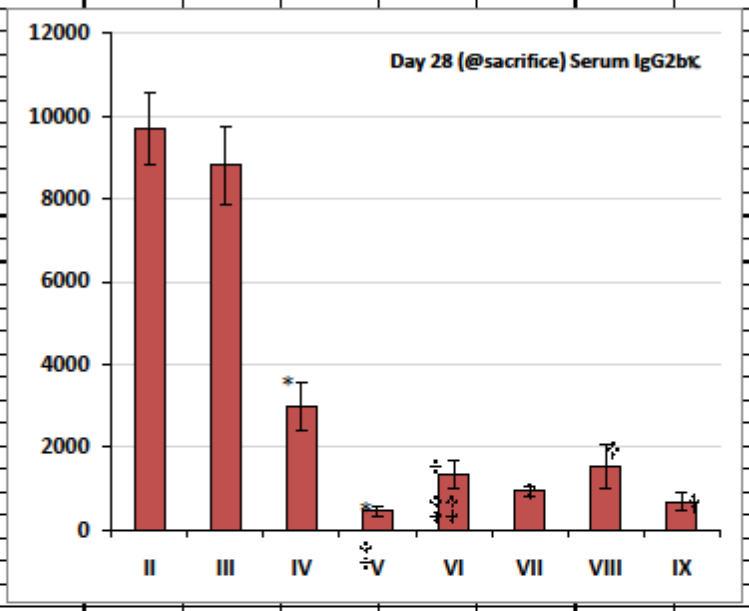


* p<0.001, vs Vehicle (Grp II)
† p<0.001, vs NP Vehicle (Grp III)
⁘ p<0.01, vs lower dose of same compound (Grp IV)
⁘⁘ p<0.05, vs same dose of Velcade (Grp IV)

**Appendex 9:** Statistical Analyses of IgG2bκ Levels in Sera from Blood Obtained at time of Sacrifice Report

## Appendix E

Statistical analyses of IgG2bκ levels in sera from blood obtained at time of sacrifice

**ANOVA Table for serum IgG (μg/ml)**

| | DF | Sum of Squares | Mean Square | F-Value | P-Value | Lambda | Power |
|---|---|---|---|---|---|---|---|
| Group | 7 | 779945109.862 | 111420729.980 | 45.429 | <.0001 | 318.001 | 1.000 |
| Residual | 53 | 129990546.298 | 2452651.817 | | | | |

**Means Table for serum IgG (μg/ml)**
**Effect: Group**

| | Count | Mean | Std. Dev. | Std. Err. |
|---|---|---|---|---|
| 1.0000 | 8 | 9693.219 | 2441.165 | 863.082 |
| 2.0000 | 8 | 8804.544 | 2648.424 | 936.359 |
| 3.0000 | 7 | 2968.020 | 1534.167 | 579.861 |
| 4.0000 | 8 | 446.229 | 375.357 | 132.709 |
| 5.0000 | 8 | 1341.231 | 915.285 | 323.602 |
| 6.0000 | 6 | 929.462 | 279.713 | 114.192 |
| 7.0000 | 8 | 1512.301 | 1491.552 | 527.343 |
| 8.0000 | 8 | 676.950 | 565.651 | 199.988 |

| | | |
|---|---|---|
| 1.0 | = Group II | Vehicle |
| 2.0 | = Group III | NP vehicle |
| 3.0 | = Group IV | Velcade 0.2mg/kg |
| 4.0 | = Group V | Velcade 1.0mg/kg |
| 5.0 | = Group VI | NP, non-targeted 0.2mg/kg |
| 6.0 | = Group VII | NP, non-targeted 1.0mg/kg |
| 7.0 | = Group VIII | NP, targeted 0.2mg/kg |
| 8.0 | = Group IX | NP, targeted 1.0mg/kg |

Fisher's PLSD for serum IgG (μg/ml)
Effect: Group
Significance Level: .1 %

| | Mean Diff. | Crit. Diff. | P-Value | |
|---|---|---|---|---|
| 1.0000, 2.0000 | 888.675 | 2727.962 | .2615 | |
| 1.0000, 3.0000 | 6725.199 | 2823.709 | <.0001 | S |
| 1.0000, 4.0000 | 9246.990 | 2727.962 | <.0001 | S |
| 1.0000, 5.0000 | 8351.987 | 2727.962 | <.0001 | S |
| 1.0000, 6.0000 | 8763.757 | 2946.536 | <.0001 | S |
| 1.0000, 7.0000 | 8180.917 | 2727.962 | <.0001 | S |
| 1.0000, 8.0000 | 9016.269 | 2727.962 | <.0001 | S |
| 2.0000, 3.0000 | 5836.524 | 2823.709 | <.0001 | S |
| 2.0000, 4.0000 | 8358.315 | 2727.962 | <.0001 | S |
| 2.0000, 5.0000 | 7463.312 | 2727.962 | <.0001 | S |
| 2.0000, 6.0000 | 7875.082 | 2946.536 | <.0001 | S |
| 2.0000, 7.0000 | 7292.242 | 2727.962 | <.0001 | S |
| 2.0000, 8.0000 | 8127.594 | 2727.962 | <.0001 | S |
| 3.0000, 4.0000 | 2521.791 | 2823.709 | .0030 | |
| 3.0000, 5.0000 | 1626.789 | 2823.709 | .0499 | |
| 3.0000, 6.0000 | 2038.558 | 3035.396 | .0231 | |
| 3.0000, 7.0000 | 1455.719 | 2823.709 | .0782 | |
| 3.0000, 8.0000 | 2291.070 | 2823.709 | .0066 | |
| 4.0000, 5.0000 | -895.002 | 2727.962 | .2582 | |
| 4.0000, 6.0000 | -483.233 | 2946.536 | .5702 | |
| 4.0000, 7.0000 | -1066.072 | 2727.962 | .1791 | |
| 4.0000, 8.0000 | -230.721 | 2727.962 | .7694 | |
| 5.0000, 6.0000 | 411.770 | 2946.536 | .6284 | |
| 5.0000, 7.0000 | -171.070 | 2727.962 | .8279 | |
| 5.0000, 8.0000 | 664.281 | 2727.962 | .4001 | |
| 6.0000, 7.0000 | -582.840 | 2946.536 | .4938 | |
| 6.0000, 8.0000 | 252.512 | 2946.536 | .7664 | |
| 7.0000, 8.0000 | 835.351 | 2727.962 | .2909 | |

Fisher's PLSD for serum IgG (μg/ml)
Effect: Group
Significance Level: 1 %

| | Mean Diff. | Crit. Diff. | P-Value | |
|---|---|---|---|---|
| 1.0000, 2.0000 | 888.675 | 2092.163 | .2615 | |
| 1.0000, 3.0000 | 6725.199 | 2165.595 | <.0001 | S |
| 1.0000, 4.0000 | 9246.990 | 2092.163 | <.0001 | S |
| 1.0000, 5.0000 | 8351.987 | 2092.163 | <.0001 | S |
| 1.0000, 6.0000 | 8763.757 | 2259.795 | <.0001 | S |
| 1.0000, 7.0000 | 8180.917 | 2092.163 | <.0001 | S |
| 1.0000, 8.0000 | 9016.269 | 2092.163 | <.0001 | S |
| 2.0000, 3.0000 | 5836.524 | 2165.595 | <.0001 | S |
| 2.0000, 4.0000 | 8358.315 | 2092.163 | <.0001 | S |
| 2.0000, 5.0000 | 7463.312 | 2092.163 | <.0001 | S |
| 2.0000, 6.0000 | 7875.082 | 2259.795 | <.0001 | S |
| 2.0000, 7.0000 | 7292.242 | 2092.163 | <.0001 | S |
| 2.0000, 8.0000 | 8127.594 | 2092.163 | <.0001 | S |
| 3.0000, 4.0000 | 2521.791 | 2165.595 | .0030 | S |
| 3.0000, 5.0000 | 1626.789 | 2165.595 | .0499 | |
| 3.0000, 6.0000 | 2038.558 | 2327.944 | .0231 | |
| 3.0000, 7.0000 | 1455.719 | 2165.595 | .0782 | |
| 3.0000, 8.0000 | 2291.070 | 2165.595 | .0066 | S |
| 4.0000, 5.0000 | -895.002 | 2092.163 | .2582 | |
| 4.0000, 6.0000 | -483.233 | 2259.795 | .5702 | |
| 4.0000, 7.0000 | -1066.072 | 2092.163 | .1791 | |
| 4.0000, 8.0000 | -230.721 | 2092.163 | .7694 | |
| 5.0000, 6.0000 | 411.770 | 2259.795 | .6284 | |
| 5.0000, 7.0000 | -171.070 | 2092.163 | .8279 | |
| 5.0000, 8.0000 | 664.281 | 2092.163 | .4001 | |
| 6.0000, 7.0000 | -582.840 | 2259.795 | .4938 | |
| 6.0000, 8.0000 | 252.512 | 2259.795 | .7664 | |
| 7.0000, 8.0000 | 835.351 | 2092.163 | .2909 | |

Fisher's PLSD for serum IgG (μg/ml)
Effect: Group
Significance Level: 5 %

| | Mean Diff. | Crit. Diff. | P-Value | |
|---|---|---|---|---|
| 1.0000, 2.0000 | 888.675 | 1570.594 | .2615 | |
| 1.0000, 3.0000 | 6725.199 | 1625.719 | <.0001 | S |
| 1.0000, 4.0000 | 9246.990 | 1570.594 | <.0001 | S |
| 1.0000, 5.0000 | 8351.987 | 1570.594 | <.0001 | S |
| 1.0000, 6.0000 | 8763.757 | 1696.435 | <.0001 | S |
| 1.0000, 7.0000 | 8180.917 | 1570.594 | <.0001 | S |
| 1.0000, 8.0000 | 9016.269 | 1570.594 | <.0001 | S |
| 2.0000, 3.0000 | 5836.524 | 1625.719 | <.0001 | S |
| 2.0000, 4.0000 | 8358.315 | 1570.594 | <.0001 | S |
| 2.0000, 5.0000 | 7463.312 | 1570.594 | <.0001 | S |
| 2.0000, 6.0000 | 7875.082 | 1696.435 | <.0001 | S |
| 2.0000, 7.0000 | 7292.242 | 1570.594 | <.0001 | S |
| 2.0000, 8.0000 | 8127.594 | 1570.594 | <.0001 | S |
| 3.0000, 4.0000 | 2521.791 | 1625.719 | .0030 | S |
| 3.0000, 5.0000 | 1626.789 | 1625.719 | .0499 | S |
| 3.0000, 6.0000 | 2038.558 | 1747.595 | .0231 | S |
| 3.0000, 7.0000 | 1455.719 | 1625.719 | .0782 | |
| 3.0000, 8.0000 | 2291.070 | 1625.719 | .0066 | S |
| 4.0000, 5.0000 | -895.002 | 1570.594 | .2582 | |
| 4.0000, 6.0000 | -483.233 | 1696.435 | .5702 | |
| 4.0000, 7.0000 | -1066.072 | 1570.594 | .1791 | |
| 4.0000, 8.0000 | -230.721 | 1570.594 | .7694 | |
| 5.0000, 6.0000 | 411.770 | 1696.435 | .6284 | |
| 5.0000, 7.0000 | -171.070 | 1570.594 | .8279 | |
| 5.0000, 8.0000 | 664.281 | 1570.594 | .4001 | |
| 6.0000, 7.0000 | -582.840 | 1696.435 | .4938 | |
| 6.0000, 8.0000 | 252.512 | 1696.435 | .7664 | |
| 7.0000, 8.0000 | 835.351 | 1570.594 | .2909 | |

**Appendix 10:** GFP-Scans

| | | Sacrifice (08/10-11/10) | | | | | | | | | | | | | | |
|---|---|---|---|---|---|---|---|---|---|---|---|---|---|---|---|---|
| | # | legs | arms | calvaria | spine | ribs | brain | heart | lungs | spleen | spleen wt (g) | kidney | ovaries | liver | body weight (g) | |
| Non-Tumor bearing ID (code) | | | | | | | | | | | | | | | | |
| Gr. I | | | | | | | | | | | | | | | | |
| | 1 | | | | | | | | | | | | | | 17.1 | |
| | 2 | | | | | | | | | | | | | | 19.7 | |
| | 3 | | | | | | | | | | | | | | 16.4 | |
| | 4 | | | | | | | | | | | | | | 18 | |
| | 5 | | | | | | | | | | | | | | 20.9 | |
| | 6 | | | | | | | | | | | | | | 18.1 | |
| 5TGM1 Tumor-bearing ID (code) | | | | | | | | | | | | | | | | |
| Gr.II VEHICLE | | | | | | | | | | | | | | | | |
| | 7 | X | X | X | X | X | | | X | X | 1.3 | | | X | 18.2 | |
| | 8 | X | X | X | X | X | | | X | X | 1.4 | | X | X | 18.2 | |
| | 9 | X | X | X | X | X | | | | X | 1.4 | | X | X | 17.4 | |
| | 10 | X | X | X | X | X | X | | X | X | 1.4 | | X | X | 19.3 | |
| | 11 | X | X | X | X | X | X | | X | X | 0.9 | | | X | 15.7 | |
| | 12 | X | X | X | X | X | | | X | X | 0.9 | | | X | 14.3 | |
| | 13 | X | X | X | X | X | | | X | X | 0.7 | | | X | 13.4 | |
| | 14 | X | X | X | X | X | | | | X | 0.9 | | | | 16.4 | fluorescent specks |
| | | | | | | | | | | | | | | | | |
| | | | | | | | | | | | | | | | | |
| Gr.III NP VEHICLE | | | | | | | | | | | | | | | | |
| | 15 | X | X | X | X | X | | | X | X | 1 | | | X | 17.1 | |
| | 16 | X | X | X | X | X | | | X | X | 1.6 | | X | X | 18.2 | |
| | 17 | X | X | X | X | X | | | X | X | 1.5 | | | X | 19.5 | |
| | 18 | X | X | X | X | X | | | X | X | 1.3 | | | X | 17.1 | Paraplegic; Tumor inside spine |
| | 19 | X | X | X | X | X | | | | X | 0.8 | | X | X | 16.7 | 4 Tumors attached to spine; 2 Tumors hip bone |
| | 20 | X | X | X | X | X | X | | X | X | 1.1 | | X | X | 16 | |
| | 21 | X | X | X | X | X | X | | X | X | 1.2 | | | X | 16.2 | |
| | 22 | X | X | X | X | X | | | X | X | 1 | | X | X | 15.5 | |

| # | legs | arms | calvaria | spine | ribs | brain | heart | lungs | spleen | spleen wt (g) | kidney | ovaries | liver | body weight (g) | |
|---|---|---|---|---|---|---|---|---|---|---|---|---|---|---|---|
| Gr.IV VELCADE 0.2 | | | | | | | | | | | | | | | |
| 23 | X | X | X | X | X | X | | X | X | 1.1 | | | X | 19.6 | light fluorescence specks |
| 24 | | X | X | X | X | | | | X | 0.7 | | | | 17.1 | |
| 25 | X | | X | X | | | | | X | 0.8 | | | | 15.5 | light fluorescence specks |
| 26 | | | | | | | | | X | 1.3 | | | | 17.8 | |
| 27 | | | | | | | | | X | 0.3 | | | | 18.9 | |
| 28 | | | | | | | | X | X | 1.4 | | X | X | 18.8 | |
| 29 | | | | | | | | | X | 0.3 | | | | 18.8 | |
| 30 | died on 7/27/10 | | | | | | | | | N/A | | | | N/A | |
| | | | | | | | | | | | | | | | |
| | | | | | | | | | | | | | | | |
| Gr.V VELCADE 1.0 | | | | | | | | | | | | | | | |
| 31 | | | | | | | | | | 0.1 | | | | 16.8 | |
| 32 | | | | | | | | | | <0.1 | | | | 12.3 | |
| 33 | | | | | | | | | | <0.1 | | | | 14.8 | |
| 34 | | | | | | | | | | 0.1 | | | | 14.7 | |
| 35 | | | | | | | | | | <0.1 | | | | 17 | |
| 36 | | | | | | | | | | 0.3 | | | | 18.5 | |
| 37 | | | | | | | | | X | 0.2 | | | | 18.2 | light fluorescence specks |
| 38 | | | | | | | | | | 0.2 | | | | 17 | |
| | | | | | | | | | | | | | | | |
| | | | | | | | | | | | | | | | |
| | | | | | | | | | | | | | | | |
| | legs | arms | calvaria | spine | ribs | brain | heart | lungs | spleen | spleen wt (g) | kidney | ovaries | liver | body weight (g) | |
| Gr.VI NP, non targeted 0.2 | | | | | | | | | | | | | | | |
| 39 | X | X | X | X | X | X | | X | X | 1.1 | | X | X | 16.4 | |
| 40 | X | X | X | X | X | X | | X | X | 0.9 | | X | X | 14.2 | |
| 41 | | | | | | | | | | < 0.1 | | | | 13.9 | |
| 42 | X | X | X | X | X | X | | | X | 1.4 | | X | X | 16.6 | |
| 43 | X | X | X | X | X | X | | X | X | 1 | | | X | 15 | Paraplegic |
| 44 | X | X | X | X | X | X | | X | X | 1.4 | | X | X | 20.3 | |
| 45 | X | X | X | X | X | X | | X | X | 1.2 | | X | X | 15.3 | |
| 46 | X | X | X | X | X | | | X | X | 1.4 | | X | X | 17.7 | |
| | | | | | | | | | | | | | | | |
| | | | | | | | | | | | | | | | |
| | | | | | | | | | | | | | | | |
| | | | | | | | | | | | | | | | |
| | | | | | | | | | | | | | | | |

| | legs | arms | calvaria | spine | ribs | brain | heart | lungs | spleen | spleen wt (g) | kidney | ovaries | liver | body weight (g) | |
|---|---|---|---|---|---|---|---|---|---|---|---|---|---|---|---|
| Gr.VII NP, non-targeted 1.0 | | | | | | | | | | | | | | | |
| 47 | X | X | X | X | X | | | | X | 0.8 | | | X | 18.3 | |
| ~~48~~ | died on 8/6/10 | | | | | | | | | N/A | | | | N/A | |
| 49 | X | X | X | X | X | | | | X | 0.7 | | | | 16.2 | light fluorescence specks |
| 50 | X | X | X | X | X | X | | | X | 1.2 | | | X | 17.4 | |
| 51 | X | X | X | X | X | X | | | X | 1.3 | | | X | 19.4 | tumor on left kidney |
| 52 | X | X | X | X | X | | | X | X | 1.2 | | | X | 13.8 | |
| ~~53~~ | died on 8/4/10 | | | | | | | | | N/A | | | | | |
| 54 | X | X | X | X | X | | | X | X | 1 | | | X | 14 | |
| | | | | | | | | | | | | | | N/A | |
| | | | | | | | | | | | | | | | |
| | | | | | | | | | | | | | | | |
| | | | | | | | | | | | | | | | |
| | legs | arms | calvaria | spine | ribs | brain | heart | lungs | spleen | spleen wt (g) | kidney | ovaries | liver | body weight (g) | |
| Gr.VIII NP, targeted 0.2 | | | | | | | | | | | | | | | |
| 55 | X | X | X | X | X | X | | X | X | 1.3 | | X | X | 20.6 | |
| 56 | X | X | X | X | X | | | X | X | 1.3 | | X | X | 19.1 | |
| 57 | X | X | X | X | X | | | | X | 0.6 | | | | 13.8 | All are light |
| 58 | X | X | X | X | X | X | | X | X | 1.1 | | X | X | 17.2 | |
| 59 | X | X | X | X | X | | | X | X | 1.1 | | X | X | 14.5 | |
| 60 | X | X | X | X | X | | | | X | 0.6 | | | | 15.4 | All are light |
| 61 | X | X | X | X | X | | | X | X | 1 | | | X | 17.9 | |
| 62 | X | X | X | X | X | | | | X | 0.9 | | | X | 16.7 | Paraplegic |
| | | | | | | | | | | | | | | | |
| | | | | | | | | | | | | | | | |
| | | | | | | | | | | | | | | | |
| Gr.IX NP, targeted 1.0 | | | | | | | | | | | | | | | |
| 63 | X | X | X | X | X | X | | X | X | 1 | | | X | 16.9 | |
| 64 | | | | | | | | | | <0.1 | | | | 15.3 | |
| 65 | | | | | | | | | X | <0.1 | | | | 13.5 | |
| 66 | X | X | X | X | X | | | | X | 0.9 | | X | X | 17 | light fluorescence specks |
| 67 | X | X | X | X | X | X | | X | X | 0.9 | | | X | 16.8 | Paraplegic |
| 68 | X | X | X | X | X | X | | | X | 0.9 | | X | X | 15.4 | |
| 69 | X | X | X | X | X | X | | X | X | 1.2 | | X | X | 18.2 | |
| 70 | X | X | X | X | X | X | | X | X | 0.9 | | X | X | 14.8 | |
| | | | | | | | | | | | | | | | |
| | | | | | | | | | | | | | | | |
| | | | | | | | | | | | | | | | |
| | | | | | | | | | | | | | | | |
| | | | | | | | | | | | | | | | |
| | | | | | | | | | | | | | | | |